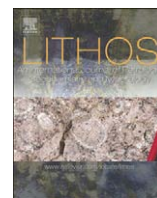




Contents lists available at ScienceDirect

Lithos

journal homepage: [www.elsevier.com/locate/lithos](http://www.elsevier.com/locate/lithos)

# The basalt-high magnesium andesite association formed by multi-stage partial melting of a heterogeneous source mantle: Evidence from Hirado-Seto, Northwest Kyushu, Southwest Japan

Hidehisa Mashima\*

New Material Research Institute Co. Ltd. Shibadai-mon 2-11-10, Minatoku, Tokyo, 105-0012, Japan

## ARTICLE INFO

## Article history:

Received 25 July 2008

Accepted 17 March 2009

Available online xxxx

## Keywords:

High magnesium andesites

Subduction zone

Multi-stage partial melting

## ABSTRACT

An association of basalts and high magnesium andesites (HMAs), erupted at 7 Ma after the opening of the Sea of Japan, exposed at Hirado-Seto in northwest Kyushu, southwest Japan. The rocks are aphyric and are characterized by enrichments in incompatible trace elements similar to those seen for oceanic island basalts, although the HMAs show a weak negative Nb anomaly. High MgO, Ni and low FeO\*/MgO indicate that the Hirado-Seto rocks were originally primitive magmas. They do not show a positive correlation between K<sub>2</sub>O/La and SiO<sub>2</sub>, or between Pb/La and SiO<sub>2</sub>, indicating that hydrous components derived from a subducting slab did not play a significant role in the genesis of the Hirado-Seto basalt–HMA magmas. Alternatively, the normative olivine–quartz–[Jd + CaTs] compositions indicate that the Hirado-Seto basalt–HMA magmas were formed by multi-stage partial melting of the source mantle at pressures ranging from 1 to 0.5 GPa along the 1300 °C mantle adiabat, assuming anhydrous conditions. Basalt magmas separated from the source mantle at 1 GPa. HMA magmas separated at 0.5 GPa. A weak negative anomaly for Nb in HMAs can be explained by precipitation of Ti–P oxides during their ascent under high *f*O<sub>2</sub> condition. Thinning of the Hirado-Seto lithosphere caused by transtensional strain during the opening of the Sea of Japan would have enabled separation of HMA magmas at unusually low pressures.

© 2009 Elsevier B.V. All rights reserved.

## 1. Introduction

The genesis of high magnesium andesite (HMA) magmas in subduction zones is one of the most important issues in earth science since their geochemical features imply that HMA magmas are candidates for parents of the continental crust (Kelemen, 1995; Rudnick, 1995). Based on seismic observations suggesting average crustal thickness of greater than 30 km (e.g., Shiomi et al., 2006), primitive melts are considered to originate within subduction zones at pressures greater than 1 GPa. High pressure melting experiments for peridotites indicate that partial melting of anhydrous peridotites form basaltic melts at pressures greater than 1 GPa (Falloon et al., 1988; Hirose and Kushiro, 1993; Kushiro, 1996; Falloon et al., 1997, 1999). On the other hand, at high pressures H<sub>2</sub>O-addition expands the olivine primary field with respect to orthopyroxene, hence hydrous peridotite could be equilibrated with HMA magmas at pressures greater than 1 GPa (Kushiro, 1969; Tatsumi, 1982; Baker and Eggler, 1987; Hirose, 1997). Therefore, slab-derived hydrous components, such as aqueous fluids and/or hydrous felsic melts, are considered to play significant roles in the genesis of HMA magmas in subduction zones.

A recent model for HMA magma genesis is the mantle/melt reaction model (Yogodzinski et al., 1994; Kelemen, 1995; Shimoda et al., 1998; Grove et al., 2002; Tatsumi and Hanyu, 2003). In this model partial melting of subducting slabs and subsequent reactions between hydrous felsic melts and the mantle form HMA magmas. Very recently, Straub et al. (2008) proposed a new slab component-induced melting (SCIM) model, in which partial melting of pyroxenite, formed by a reaction between slab-derived fluids and peridotite, generates HMA magmas.

HMAs are generally associated with basalts forming a basalt–HMA association (e.g., Kay, 1978; Tatsumi, 1982; Grove et al., 2002; Bourdon et al., 2003). Early in the history of the debate on HMA magma genesis, Tomita (1958) pointed out that a petrologic model for the genesis of HMA magmas should also explain the genesis of basalt magmas associated with them. Results of high pressure melting experiments on hydrous peridotite (Hirose and Kawamoto, 1995; Hirose, 1997), however, indicate that the SCIM models cannot resolve Tomita's proposition.

Previous SCIM models assume that both HMA and basalt magmas separated from their source mantle at the same pressures, greater than 1 GPa. Partial melts obtained from hydrous melting experiments of a peridotite (KLB-1) at 1050 °C and 1 GPa were HMAs (Hirose, 1997). Those obtained above 1200 °C were basalts (Hirose and Kawamoto, 1995). A temperature difference greater than 150 °C exists

\* Tel.: +81 3 6410 5471; fax: +81 3 6410 5472.

E-mail address: [hisa.mashima@mbn.nifty.com](mailto:hisa.mashima@mbn.nifty.com).

between basalts and HMA magmas at 1 GPa even under hydrous conditions. If the starting material is anhydrous, the temperature of a basaltic partial melt with 10 wt.% MgO is 1300 °C (Hirose and Kushiro, 1993), indicating that the temperature difference between basalt magmas and HMA magmas expands to greater than 250 °C. Taking into account the latent heat effects during partial melting and heat conduction in the mantle, the temperature difference between hydrous HMAs and basalts is too large for the mantle to remain at the same pressure. Therefore, SCIM models need a mechanism that creates a large temperature variation in the mantle at an identical pressure. Such a mechanism is the most important issue relative to the SCIM model for HMA magma genesis (Shimoda et al., 1998).

Results of high pressure melting experiments indicate that partial melting of anhydrous mantle at pressures less than 1 GPa could form HMA magmas (Jaques and Green, 1980; Jenner, 1982; Tatsumi, 1982; Falloon et al., 1988; Kushiro, 1996). Falloon et al. (1988) proposed a multi-stage partial melting (MSPM) model for basalt–HMA associations in subduction zones. They proposed that HMA magmas were separated from the source mantle at pressures less than 1 GPa, and that basalt magmas associated with HMAs were separated from the source at pressures greater than 1 GPa. They also suggested that MSPM could form a basalt–HMA association along a mantle adiabat. Earth scientists, however, have given little attention to the MSPM model, because the model needs abnormally shallow Moho depths for

HMA magma separation in subduction zones. Geological, geophysical and rheological studies, however, indicate that crustal thickness could dramatically change through tectonic activities, such as back-arc extension and intra-arc basin formation, in subduction zones (e.g., Wernicke, 1985; Zhou et al., 1989; Nakada et al., 1997; Yamada and Nakada, 2006).

Basalt–HMA associations erupted from 10 to 6 Ma are found in northwest Kyushu, SW Japan (Matsumoto, 1961; Yamaguchi, 1964). Typical NW Kyushu basalts do not have geochemical features suggesting contributions of slab components to their magma genesis. Their geochemical features are similar to those of OIBs (e.g., Uto et al., 2004). Thus, the genesis of NW Kyushu basalt–HMA associations would give us new insights into the genesis of basalt–HMA associations in subduction zones. In this paper, I discuss the genesis of the Hirado-Seto basalt–HMA association in NW Kyushu. First, I present the tectonic and petrologic background for the Hirado-Seto volcanism. Various lines of evidence indicate that Hirado-Seto was subject to strong transtensional strain during the opening of the Sea of Japan prior to the volcanism. Second, I present the petrology and geochemistry of the Hirado-Seto samples. Petrologic features, such as high MgO and low FeO\*/MgO, indicate that the Hirado-Seto samples were originally primitive melts. Geochemical features, such as the absence of a positive correlation between K<sub>2</sub>O/La and SiO<sub>2</sub>, indicate that slab-derived hydrous components did not play a significant role

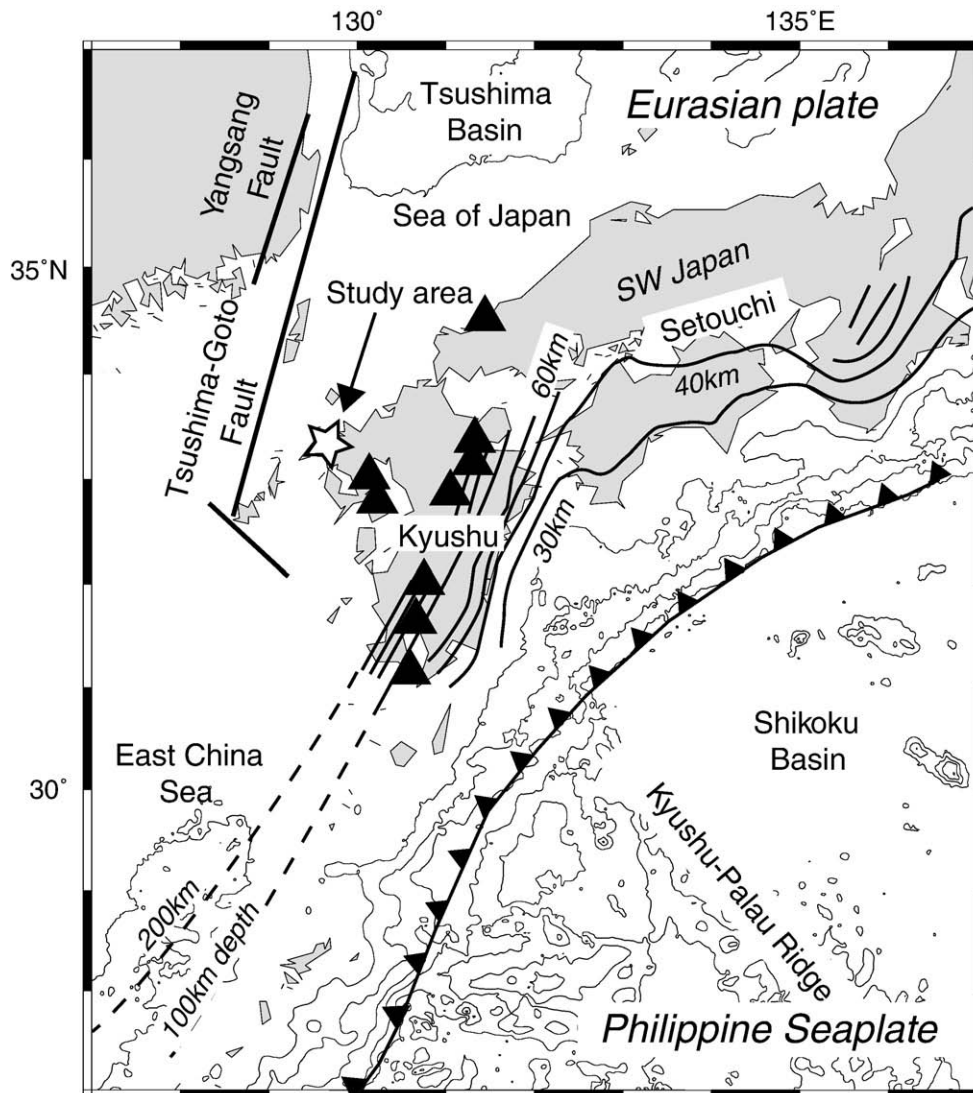
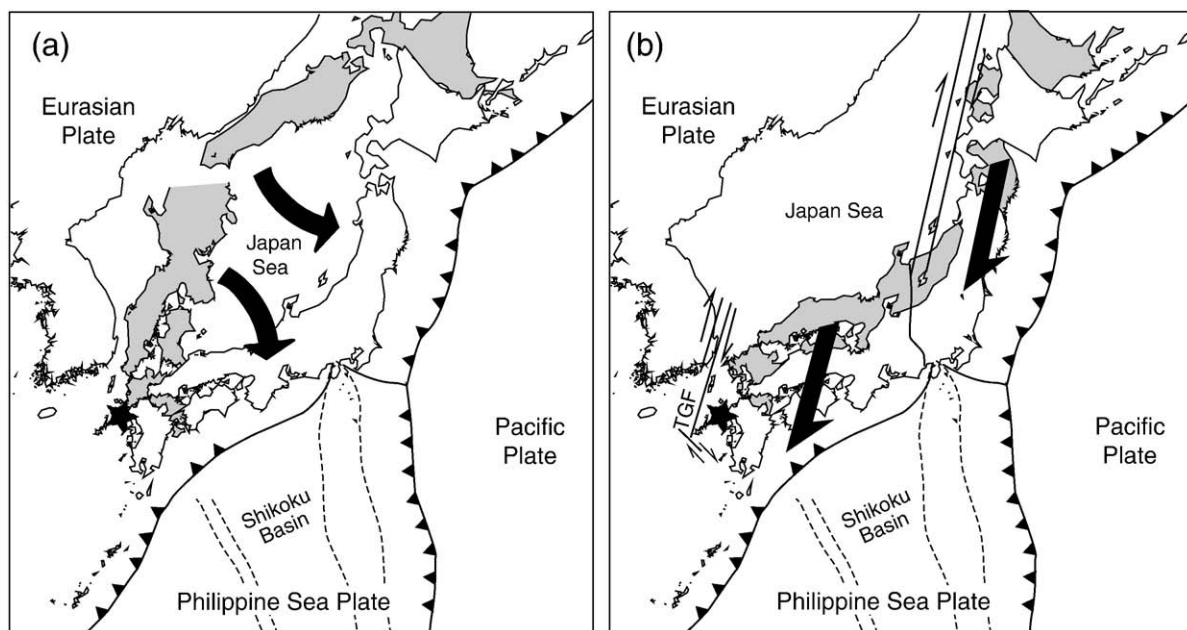


Fig. 1. Map showing the tectonic setting of southwest Japan. The depth of the subducting slab is from Ishida and Sakanashi (2003). Solid triangles are active volcanos. Open Star is the study area.



**Fig. 2.** Two types of opening models for the Sea of Japan. (a) Double-door opening model (e.g. Tatsumi and Hanyu, 2003), which indicates that NW Kyushu was subject to a strong horizontal compressive stress field. (b) Pull-apart opening model (e.g. Mashima, 2008b), which indicates that NW Kyushu was subject to a strong transtensional stress field. TGF is the Tushima-Goto Fault.

in the magma genesis. Third, I examine the genesis of the Hirado-Seto basalt–HMA association. Major element and trace element features indicate that MSPM occurred at pressures ranging from 1 to 0.5 GPa. The tectonic history, such as strong transtensional tectonics that could cause crustal thinning during the opening of the Sea of Japan, are consistent with this assumption. Finally, I consider the global significance of the MSPM model.

## 2. Tectonic and geologic backgrounds

NW Kyushu is located in a subduction zone where the Philippine Sea plate meets the Eurasian plate (Fig. 1). The Philippine Sea plate

subducting there is composed of the young oceanic lithosphere of the Shikoku Basin. Partial melting of the subducting Shikoku Basin is considered to have played an essential role in the genesis of HMA magmas at Setouchi, SW Japan (Shimoda et al., 1998; Tatsumi et al., 2001, 2003; Tatsumi and Hanyu, 2003; Kimura et al., 2005). The Shikoku Basin shows a contrasting configuration between Kyushu and Setouchi. The basin gently subducts at Setouchi. On the other hand, it steeply subducts at Kyushu, and then vertically descends into the mantle on the oceanic side of the volcanic front of Kyushu (e.g., Ishida and Sakanashi, 2003; Wang et al., 2004).

Prior to the basalt–HMA magmatism in NW Kyushu, the Sea of Japan opened from 23 to 15 Ma (Jolivet et al., 1994). Related to the

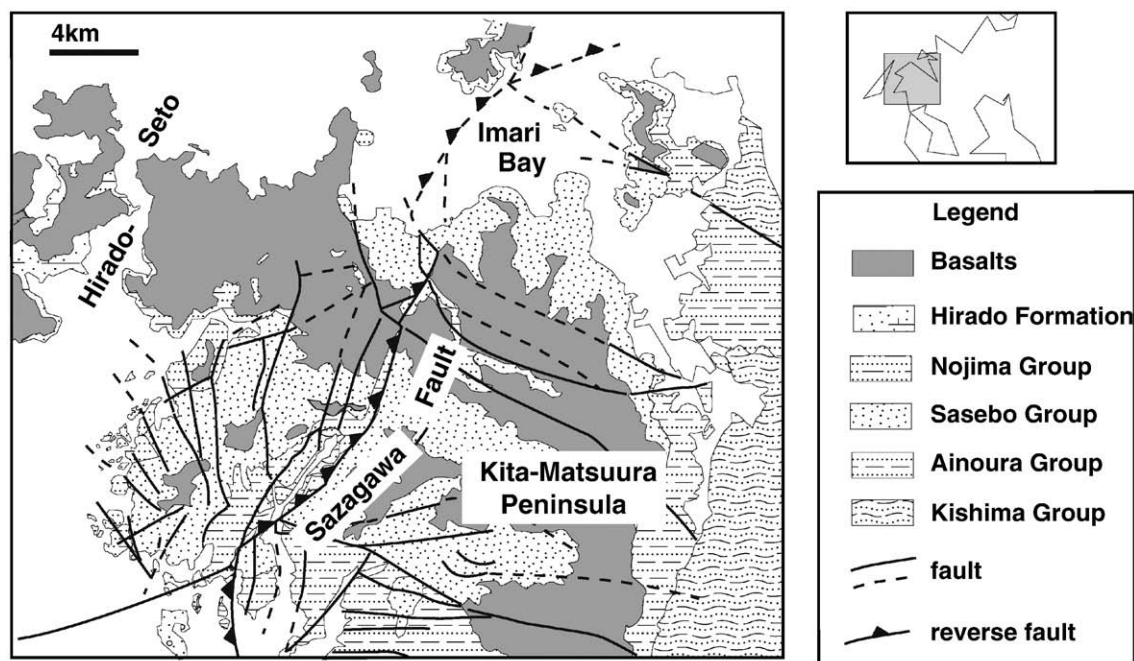


**Fig. 3.** Geological map of the Kita-Matsuura Peninsula (Matsui et al., 1989).

**Table 1**  
Chemical compositions of olivine phenocrysts in Hirado-Seto samples.

	Basalt (KM78)			HMA (KM67)		
	Core			Core		
MgO (wt.%)	46.74	44.17	43.11	43.98	43.35	43.34
SiO <sub>2</sub>	44.29	44.44	43.88	43.27	43.25	42.64
FeO	8.98	11.39	13.01	12.75	13.40	14.03
Total	100.00	100.00	100.00	100.00	100.00	100.00
Mg	1.681	1.604	1.578	1.611	1.592	1.599
Si	1.069	1.082	1.078	1.063	1.066	1.055
Fe	0.181	0.232	0.267	0.262	0.276	0.290
Total	2.931	2.918	2.922	2.937	2.934	2.945
O	4.000	4.000	4.000	4.000	4.000	4.000
Fo	90.3	87.4	85.5	86.0	85.2	84.6

genesis of the Setouchi HMAs, Tatsumi and coworkers adopted the double door-opening model for the Sea of Japan (Shimoda et al., 1998; Tatsumi and Hanyu, 2003; Tatsumi et al., 2003). In the double door-opening model, SW Japan rotated 60° clockwise during the opening of the Sea of Japan (Fig. 2a). The model, however, is based only on paleomagnetic data indicating clockwise declinations of spheric Fe–Ti oxide minerals in analyzed samples from SW Japan. It is inconsistent with geologic relationships between SW Japan, Eurasia and the East China Sea (Ichikawa, 1972; Inoue, 1982). Right-lateral transtensional structures of the Tsushima-Goto Fault indicate that SW Japan displaced along the fault with a strike-slip manner during the opening of the Sea of Japan (Fig. 2b) (Itoh, 2001; Mashima, 2008b).

Seismic observations indicate that the present day NW Kyushu crust is ca. 30 km thick (Murakoshi, 2003). Previous petrologic studies of mantle xenoliths found in the NW Kyushu basalts indicate that the thick NW Kyushu lithosphere of the present day was newly formed through cooling and inversion tectonics in the post opening period of the Sea of Japan. Na<sub>2</sub>O of pyroxenes in peridotite xenoliths is lower than 0.6 wt.%, indicating that the peridotite xenoliths are low-pressure mantle restites (Arai et al., 2001). NW Kyushu basalts younger than 4 Ma contain mantle xenoliths. Basalts older than 6 Ma contain only ultramafic xenocrysts (Ishibashi, 1970). The floor of the Sea of Japan was tightly folded in a NE–SW direction during the inversion tectonics between 8 and 5 Ma. The lithosphere of the back-arc and inner-arc of SW Japan is considered to have been significantly shortened during this process (Itoh and Nagasaki, 1996).

The samples analyzed in this study were collected from Hirado-Seto at the western end of the Kita-Matsuura Peninsula (Fig. 3). The basement rocks of Hirado-Seto belong to the Nojima Group and the Hirado Formation. The Nojima Group is composed of sandstones, mudstones and pyroclastics deposited in freshwater during the opening of the Sea of Japan. The Hirado Formation is composed of sandstones and mudstones deposited after the Nojima Group. The Nojima Group deposition is characterized by a high subsidence ratio of at least 500 m/My (Komatsubara et al., 2005).

A geochronologic study suggests that the Hirado-Seto volcanism occurred at 7–6.5 Ma (Uto et al., 2004). Uto et al. (2004) proposed that the Hirado-Seto volcanism was caused by lithospheric extension after the opening of the Sea of Japan. Their interpretation, however, is inconsistent with the geologic evidence. As mentioned above, NW Kyushu was subject to a strong horizontal compressive stress oriented NW–SE in late Miocene. The Sazagawa Fault striking to NE–SW in the Kita-Matsuura Peninsula acted as a reverse fault and displaced basalt lava flows at that time (Kurasawa, 1970). These lines of evidence indicate that the Hirado-Seto volcanism occurred under a horizontal compressive stress field oriented in a NW–SE direction.

### 3. Analytical methods

Chemical compositions of olivine phenocrysts and spinel inclusions were determined by Scanning Electron Microscopy (SEM)

(Simadzu SS-550S combined with an Energy Dispersive X-ray (EDX) system Genesis 2000AY) at the Center of Advanced Instrumental Analysis, Kyushu University. The accelerating potential, specimen current and analytical time were, 20 kV, 5 nA and 200 s. ZAF correction procedures were employed. Major elements, Ni, Cr, and V were determined by X-ray Fluorescence (XRF) using a Rigaku System 3270E unit at the Tono Geoscience Center, Japan Atomic Energy Agency. An Rh anode tube, operating at 50 kV and 50 mA, was used for determination. 1 g of powdered rock, 5 g of Li<sub>2</sub>B<sub>4</sub>O<sub>7</sub> and 0.2 g of 80% Lil solution were mixed and fused in a radio high frequency furnace to form a homogeneous glass disk. Calibrations were carried out using synthetic samples. Standard samples for major element analyses were made from chemical reagents. High-purity SiO<sub>2</sub> was used for the major element matrix for the standard glasses used for trace element analyses.

Trace elements, other than Ni, Cr and V, were determined by Inductively Coupled Plasma–Mass Spectrometry (ICP-MS) using an SII SPX 9200 mass spectrometer at the Tono Geoscience Center. Radio frequency power was 1.2 kW. 0.1 g of powdered rock was weighed in a 30 ml PFA vessel. 1 ml of 1 ppm In solution was added as an internal standard for determination. A sample was decomposed using 1 ml HF + 1 ml HNO<sub>3</sub>. At first, decomposition was operated at an open system to release SiF<sub>4</sub> formed through initial decomposition. After the release of SiF<sub>4</sub>, the vessel was sealed with a PFA screw-cap and kept at 100 °C overnight for further decomposition. The vessel was, then, opened and 1 ml HClO<sub>4</sub> was added. Stepwise heating from 150 to 210 °C was carried out to avoid oxide formation. During heating, the vessel was shaken to release HF. After fuming stopped, a decomposed sample was cooled to room temperature, then 10 ml 1 M HNO<sub>3</sub> was added to dissolve decomposed residues. The PFA vessel was lit up from its bottom and sidewall to check complete dissolution. After confirmation of complete decomposition, a sample solution was filled up to 100 ml with H<sub>2</sub>O.

### 4. Analytical results

The Hirado-Seto samples are generally aphyric and contain less than 5 vol.% phenocryst minerals (Table 3). Olivine phenocrysts have various shapes. Both euhedral and anhedral olivines are observed, indicating various origins for the olivine phenocrysts. Chemical composition of olivine phenocrysts are characterized by high MgO/(MgO + FeO) ranging from 0.90 to 0.84 (Table 1). Spinel inclusions are found in the olivine phenocrysts. Cr# = Cr/(Cr + Al) of andesite

**Table 2**  
Chemical compositions of spinel inclusions in olivine phenocrysts.

	Basalt (KM78)			HMA (KM67)		
	Inc.			Inc.		
MgO (wt.%)	17.15	13.38	11.96	12.39	12.70	9.72
Al <sub>2</sub> O <sub>3</sub>	49.82	37.31	29.90	26.16	26.72	13.56
TiO <sub>2</sub>	0.57	4.15	3.69	0.63	0.66	7.96
V <sub>2</sub> O <sub>5</sub>	0.16	0.31	0.34		0.24	0.66
Cr <sub>2</sub> O <sub>3</sub>	15.72	18.63	22.42	34.67	33.37	29.31
FeO	16.58	26.23	31.70	26.14	25.74	38.80
Total	100.00	100.01	100.01	99.99	99.43	100.01
Mg	0.690	0.575	0.533	0.559	0.573	0.469
Al	1.585	1.269	1.053	0.934	0.954	0.517
Ti	0.012	0.090	0.083	0.014	0.015	0.194
V	0.003	0.006	0.007		0.005	0.014
Cr	0.335	0.425	0.530	0.830	0.799	0.750
Fe <sup>2+</sup>	0.050	0.114	0.237	0.207	0.207	0.315
Fe <sup>3+</sup>	0.324	0.519	0.555	0.455	0.445	0.735
Total	2.999	2.998	2.998	2.999	2.998	2.994
O	4.000	4.000	4.000	4.000	4.000	4.000
Cr/(Cr+Al)	0.175	0.251	0.335	0.471	0.456	0.592
Mg/(Mg+Fe <sup>2+</sup> )	0.681	0.526	0.490	0.551	0.563	0.390
Fe <sup>3+</sup> /(Cr+Al+Fe <sup>3+</sup> )	0.026	0.063	0.130	0.105	0.106	0.199
Fo of host olivine	90	87	86	86	86	84

ranges from 0.44 to 0.59, higher than that for basalts which range from 0.18 to 0.34 (Table 2).

Bulk rock compositions of the analyzed samples are reported in Table 3. SiO<sub>2</sub> in Hirado-Seto samples range from 49.5 to 56.5 wt.%. They have high MgO (5–8.5 wt.%) and low FeO\*/MgO (0.9–1.7). High MgO and low FeO\*/MgO of the andesites indicate that they are high magnesium andesites (HMAs). Major element oxides are plotted against SiO<sub>2</sub> in Fig. 4. MgO and FeO\*/MgO show positive and negative correlations, respectively, with SiO<sub>2</sub>. TiO<sub>2</sub> ranges from 0.9 to 2.3 wt.%, Al<sub>2</sub>O<sub>3</sub> from 13.5 to 17 wt.%, Fe<sub>2</sub>O<sub>3</sub>\* from 8.5 to 12 wt.%, MnO from 0.14 to 0.2 wt.%, CaO from 7 to 9 wt.%, and P<sub>2</sub>O<sub>5</sub> from 0.1 to 0.65 wt.%. These elements show negative correlations with SiO<sub>2</sub>. Na<sub>2</sub>O and K<sub>2</sub>O range from 2.5 to 3.5 wt.% and from 0.5 to 2.5 wt.%. They do not show a systematic relationship with SiO<sub>2</sub>.

Compatible trace elements are plotted against SiO<sub>2</sub> in Fig. 5. The Hirado-Seto samples contain Ni = 55–219 ppm, Cr = 90–453 ppm. High Ni and Cr contents characterize the samples. Ni and Cr show positive correlations with SiO<sub>2</sub>. V and Sr range from 101 to 189 ppm and from 328 to 698 ppm. They show negative correlations with SiO<sub>2</sub>. V/Nd and Sr/Nd, however, do not show any systematic correlation with SiO<sub>2</sub>.

The relative abundances of incompatible trace elements are shown in Fig. 6. With respect to primitive mantle, the Hirado-Seto samples have incompatible element enriched patterns. HMA samples show weak negative Nb anomalies. Almost all the basalts do not show a negative Nb anomaly. The variations of Nb/La, K<sub>2</sub>O/La and Pb/La

against SiO<sub>2</sub> are shown in Fig. 7. Samples with SiO<sub>2</sub> = 49.5–53.6 wt.% have relatively constant Nb/La = 0.7–1.06, although a basalt sample has Nb/La = 0.5. Nb/La of HMAs is 0.6, which is a little smaller than that of the other samples. K<sub>2</sub>O/La, ranging from 215 to 475, does not show a systematic correlation with SiO<sub>2</sub>. K<sub>2</sub>O/La in the HMAs is similar to that in the basalts. The Pb/La ratio is relatively constant at 0.02–0.04, except for a basalt sample with Pb/La = 0.06, and there is no systematic relationship with SiO<sub>2</sub>.

## 5. Discussion

### 5.1. Primitive natures of Hirado-Seto samples

Hirado-Seto samples show a large variation in SiO<sub>2</sub> ranging from 49.5 to 56.5 wt.%. The large variation in SiO<sub>2</sub> in volcanic rocks from the Kita-Matsuura Peninsula has been considered to be caused by magmatic processes in the crust (Kurasawa, 1967; Kakubuchi et al., 1994; Yanagi and Maeda, 1998). Yanagi and Maeda (1998) proposed that basaltic andesites from Kita-Matsuura were formed by mixing between basalt and andesite magmas. The andesite endmember for magma mixing was formed by fractional crystallization of olivine + cpx + plagioclase + Fe–Ti oxides. Their model was based only on major element data and is inconsistent with the trace element results for the Hirado-Seto samples.

Yanagi and Maeda (1998) proposed that fractional crystallization of Fe–Ti oxides, plagioclase, olivine and clinopyroxene played an

**Table 3**  
Bulk rock compositions of Hirado-Seto rocks.

	KM52	KM53	KM54	KM55	KM66	KM67	KM68	KM71	KM73	KM74	KM75	KM76	KM77	KM78	KM93
SiO <sub>2</sub> (wt.%)	52.75	50.72	49.80	51.29	56.41	56.50	53.62	52.32	52.01	53.49	51.50	50.50	50.45	49.82	49.63
TiO <sub>2</sub>	1.46	1.34	2.24	1.57	0.85	0.86	1.33	1.36	1.64	1.32	1.48	1.89	1.87	2.13	2.25
Al <sub>2</sub> O <sub>3</sub>	15.38	14.82	17.21	14.95	13.79	13.77	15.59	15.45	15.72	14.98	16.63	15.81	15.70	15.60	17.16
Fe <sub>2</sub> O <sub>3</sub> *	9.54	11.31	10.32	11.73	8.63	8.58	9.43	10.08	12.04	10.75	10.38	11.64	11.89	11.73	10.70
MnO	0.17	0.17	0.17	0.18	0.14	0.14	0.16	0.18	0.16	0.17	0.19	0.17	0.18	0.19	0.20
MgO	7.60	8.48	6.25	7.51	8.35	8.34	6.92	7.17	6.23	7.22	6.90	6.61	6.62	6.70	5.92
CaO	8.57	9.18	7.58	8.39	7.31	7.32	7.12	7.73	8.34	8.01	7.43	9.16	8.86	8.77	7.40
Na <sub>2</sub> O	2.82	2.63	3.14	2.82	2.60	2.64	3.59	3.17	2.88	2.87	3.28	2.80	2.81	3.14	3.15
K <sub>2</sub> O	1.32	0.68	2.62	0.89	1.70	1.63	1.76	1.74	0.90	1.03	1.39	0.74	0.94	1.27	2.57
P <sub>2</sub> O <sub>5</sub>	0.33	0.22	0.64	0.28	0.17	0.18	0.47	0.44	0.27	0.25	0.53	0.38	0.38	0.44	0.66
Total	99.94	99.55	99.97	99.61	99.95	99.96	99.99	99.64	100.19	100.09	99.71	99.70	99.70	99.79	99.64
FeO*/MgO	1.13	1.20	1.49	1.41	0.93	0.93	1.23	1.27	1.74	1.34	1.35	1.58	1.62	1.58	1.63
Nb (ppm)	21.0	11.2	49.7	13.6	19.1	19.4	39.4	39.6	11.2	15.4	40.4	16.2	15.1	17.6	49.9
Zr	166	104	291	124	115	114	273	252	110	134	277	114	111	151	294
Y	23.7	19.3	25.6	23.2	19.6	19.8	23.0	22.0	26.6	22.4	27.7	22.9	22.4	26.8	26.2
Sr	420	350	698	386	359	361	523	559	397	328	585	456	439	565	626
Rb	29.5	11.4	71.8	17.8	48.1	45.0	40.8	40.0	17.9	24.2	24.2	12.5	20.6	19.1	62.1
V	149	145	160	150	104	101	103	134	163	126	102	164	154	189	159
Cr	306	410	94	274	448	453	316	450	227	295	308	200	184	164	90
Ni	142	127	64	128	216	219	183	208	67	147	196	86	76	81	55
Ba	352	270	689	216	471	455	725	875	187	258	748	275	263	257	700
La	26.1	15.8	46.5	17.5	32.5	32.1	46.0	46.0	22.3	20.2	53.6	18.3	17.7	22.4	48.1
Ce	53.3	32.0	92.8	37.5	54.8	52.3	79.6	80.0	36.5	40.4	82.5	39.0	37.8	54.0	96.4
Pr	6.2	3.7	11.0	4.6	5.5	5.3	8.6	8.6	7.2	4.8	10.0	4.6	4.4	6.8	11.5
Nd	25.9	15.9	43.1	19.9	20.0	19.3	32.2	32.0	30.6	19.6	37.6	19.8	19.6	29.7	44.9
Sm	5.3	3.8	7.8	4.6	3.8	3.6	5.8	6.0	7.1	4.4	6.8	4.6	4.5	6.3	8.1
Eu	1.6	1.3	2.2	1.5	1.2	1.2	2.0	1.9	2.2	1.5	2.2	1.6	1.6	1.9	2.3
Gd	5.1	4.1	6.5	4.8	3.8	3.7	5.4	5.4	6.4	4.7	6.7	4.9	4.9	6.2	6.9
Tb	0.76	0.65	0.89	0.70	0.61	0.62	0.80	0.81	1.02	0.75	0.96	0.77	0.76	0.92	0.99
Dy	4.6	4.0	5.3	4.3	3.7	3.6	4.6	4.5	5.7	4.4	5.4	4.4	4.4	5.3	5.4
Ho	0.92	0.79	0.97	0.88	0.74	0.72	0.88	0.90	1.1	0.88	1.1	0.87	0.84	1.0	1.0
Er	2.5	2.2	2.7	2.4	2.0	2.0	2.4	2.5	2.8	2.4	2.9	2.3	2.3	2.8	2.7
Tm	0.35	0.30	0.37	0.33	0.31	0.30	0.36	0.37	0.40	0.35	0.44	0.34	0.33	0.41	0.40
Yb	2.2	1.9	2.3	2.0	1.9	1.9	2.2	2.2	2.4	2.2	2.7	2.0	1.9	2.4	2.3
Lu	0.33	0.27	0.31	0.29	0.30	0.30	0.36	0.35	0.36	0.33	0.42	0.31	0.31	0.38	0.37
Hf	4.1	2.7	6.6	3.3	3.0	2.9	5.6	5.5	3.0	3.4	5.9	2.8	2.7	3.7	6.7
Ta	2.2	1.5	3.7	1.4	2.1	1.9	3.1	2.3	1.3	1.9	3.8	1.7	1.6	1.7	4.3
Pb	0.96	0.54	1.5	0.68	1.3	1.2	1.1	1.0	0.71	0.76	1.2	0.57	0.56	1.3	1.6
U	0.69	0.42	1.2	0.44	1.6	1.5	1.5	1.7	0.44	0.74	1.4	0.48	0.48	0.48	1.2
Th	3.5	2.3	6.8	2.4	7.4	7.2	7.3	8.1	2.4	3.5	6.9	2.3	2.3	2.6	7.3
Modal olivine (vol.%)	4.9	4.8	2.7	4.5	3.3	4.4	3.1	5.2	4.2	3.0	3.2	4.1	3.6	4.5	5.0

essential role in the  $\text{SiO}_2$  variation. Ni and Cr are compatible elements with respect to Fe–Ti oxides and should show negative correlations with  $\text{SiO}_2$ . However, Ni and Cr show positive correlations with  $\text{SiO}_2$ . If fractionation of plagioclase played a significant role in the andesite magma genesis, Sr/Nd should show a negative correlation with  $\text{SiO}_2$ . However, Sr/Nd of the Hirado-Seto samples, does not show a systematic correlation with  $\text{SiO}_2$  (Fig. 5), indicating that significant fractionation of plagioclase did not occur in the Hirado-Seto magmas. These trace element features of the Hirado-Seto samples, therefore, indicate that the interpretation of Yanagi and Maeda (1998) does not explain the genesis of the Hirado-Seto magmas. Also, the Ni contents

of the HMAs are higher than those of the basalts, indicating that fractionation of the basalt magmas could not form the HMA magmas.

Alternatively, Mashima (2005) proposed that partial melting of the source mantle essentially controlled the compositional variations of the NW Kyushu basalts. Major element and compatible trace element features of the Hirado-Seto basalt–HMA association are consistent with this interpretation.

High MgO, Ni and low  $\text{FeO}^*/\text{MgO}$  indicate that both basalts and HMAs were originally primitive magmas. Fig. 8 shows Mg–Fe–Ni compositions of calculated olivine in equilibrium with the Hirado-Seto samples. Fo and NiO contents of calculated olivines range from 81.3 to

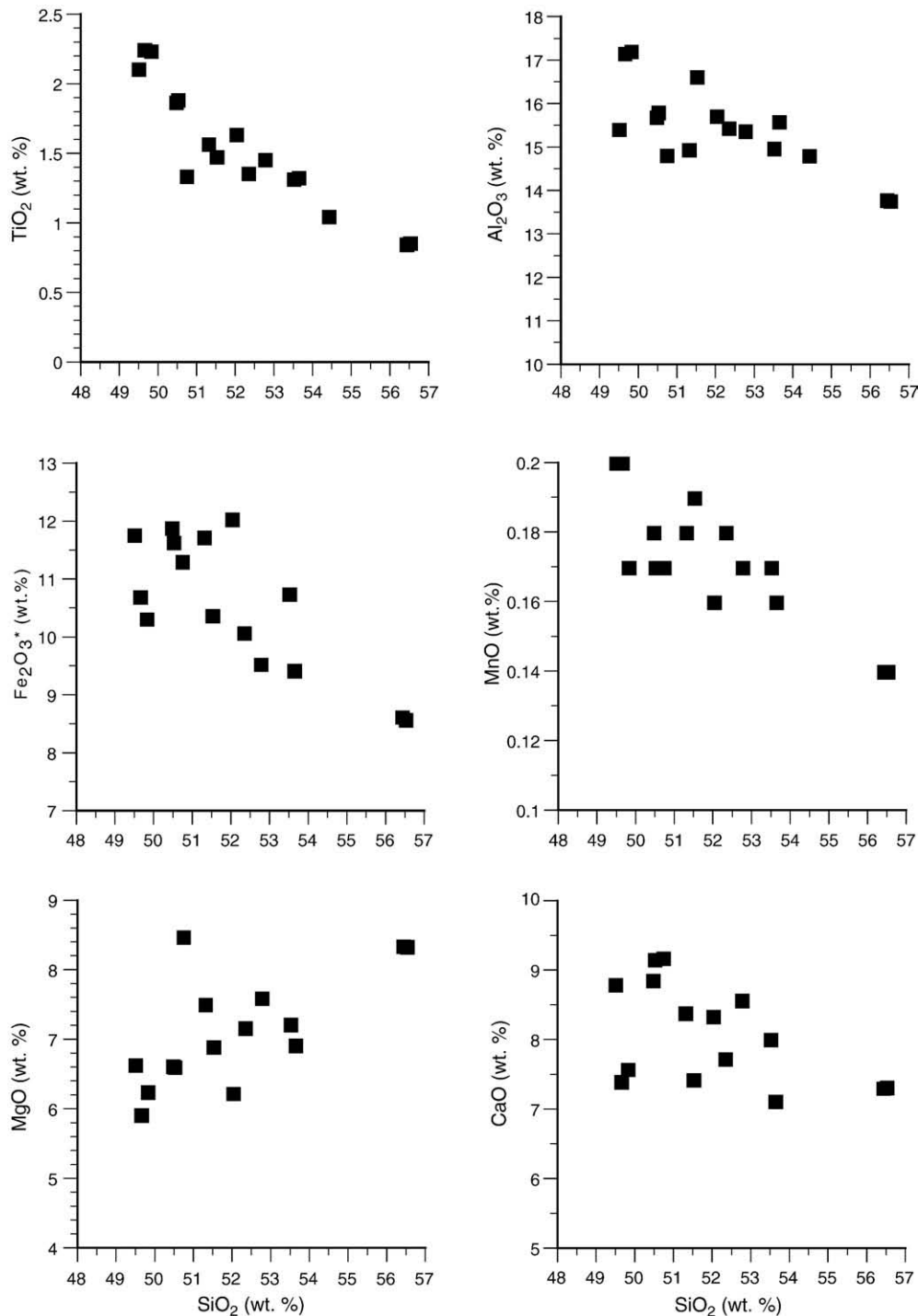


Fig. 4. Major element variations of Hirado-Seto samples.

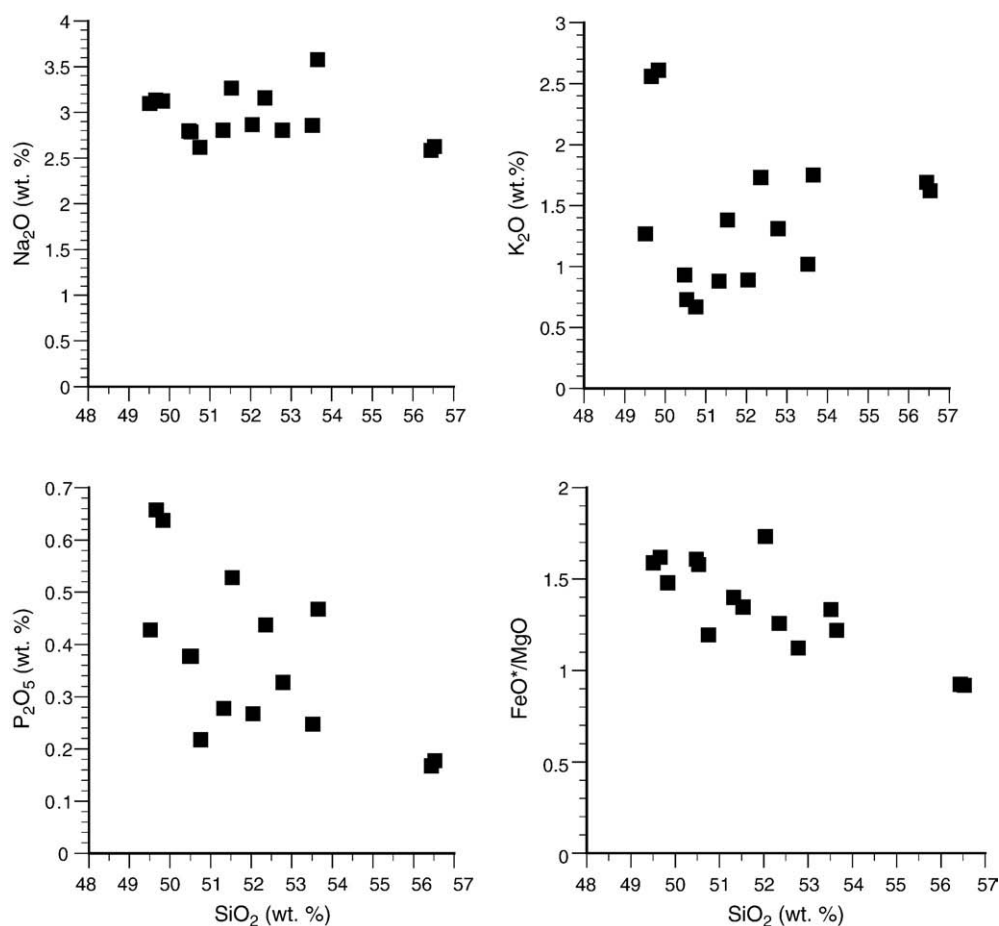


Fig. 4 (continued).

89.2 and from 0.14 to 0.47 wt.%, respectively. Calculated olivines have Mg–Fe–Ni compositions of mantle olivines (Sobolev et al., 2005) although some of them are outside of mantle olivine compositions. The Mg–Fe–Ni compositions of the Hirado-Seto samples, therefore, indicate that these magmas were originally equilibrated with the mantle.

For a transitional sample (KM68), the MgO/(MgO + FeO) ratio of the host melt calculated from olivine phenocryst compositions is higher than that expected from the bulk rock composition (Fig. 9). Since the olivine xenocrysts are magnesian, they were apparently derived from a dunite layer of the uppermost part of the mantle. Because of the aphyric nature of KM68, the effects of olivine xenocrysts on bulk rock composition would be negligible. MgO/(MgO + FeO) ratios of olivines in a HMA (KM66) are lower than that for an olivine equilibrated with the bulk rock composition. This would be the result of resorption of orthopyroxene which crystallized earlier than olivine during magma ascent. Since the orthopyroxene primary phase field expands with respect to that of olivine at high pressure, HMA magmas would initially crystallize orthopyroxene. Orthopyroxene phenocrysts in HMA magmas would have resolved during magma ascent because the orthopyroxene field shrinks with decreasing pressure.

## 5.2. Testing of the SCIM models

Seismic observations indicate that average thickness of the crust would be greater than 30 km in subduction zones (e.g., Shiomi et al., 2006). Results of previous melting experiments indicate that partial melting of anhydrous peridotites could not form andesite melts at pressure greater than 1 GPa (Jaques and Green, 1980; Falloon et al.,

1988; Hirose and Kushiro, 1993; Falloon et al., 1997). On the other hand, H<sub>2</sub>O at high pressure expands the olivine primary field with respect to the orthopyroxene field, indicating that hydrous melting of a peridotite could form andesite melts at pressure greater than 1 GPa (Kushiro, 1969; Tatsumi, 1982; Hirose, 1997). Therefore, hydrous components such as melts or aqueous fluids derived from subducting slabs are generally believed to cause HMA magmatism in subduction zones (e.g., Yogodzinski et al., 1994; Kelemen, 1995; Shimoda et al., 1998; Grove et al., 2002; Tatsumi and Hanyu, 2003).

Based on geochemical studies, Tatsumi and coworkers suggested that a reaction between the mantle and slab-derived felsic melts formed the Setouchi basalt–HMA associations in SW Japan (Shimoda et al., 1998; Tatsumi et al., 2001, 2003; Tatsumi and Hanyu, 2003). In their model, basalts associated with HMAs were derived from a mantle less metasomatized by slab-derived felsic melts. Grove et al. (2002) discussed the origin of the basalt–HMA association from Mt. Shasta, North California based on melting experiments. They assumed that slab-derived hydrous components cause extensive hydrous melting of the wedge mantle, and that HMA magmas were formed by a reaction between the mantle and the hydrous basalt melts. These models assume that both basalt and HMA magmas were separated from the source mantle at pressures greater than 1 GPa. Major element and trace element features of the Hirado-Seto basalt–HMA association, however, indicate that SCIM models are inadequate to explain their petrogenesis.

The SCIM model requires a large temperature variation in the mantle at the same pressure to form a basalt–HMA association (Shimoda et al., 1998; Mashima, 2008a). Melting experiments on peridotite (KLB-1) under hydrous conditions at 1 GPa suggest that the temperature of hydrous HMAs with SiO<sub>2</sub> > 55 wt.% would be lower

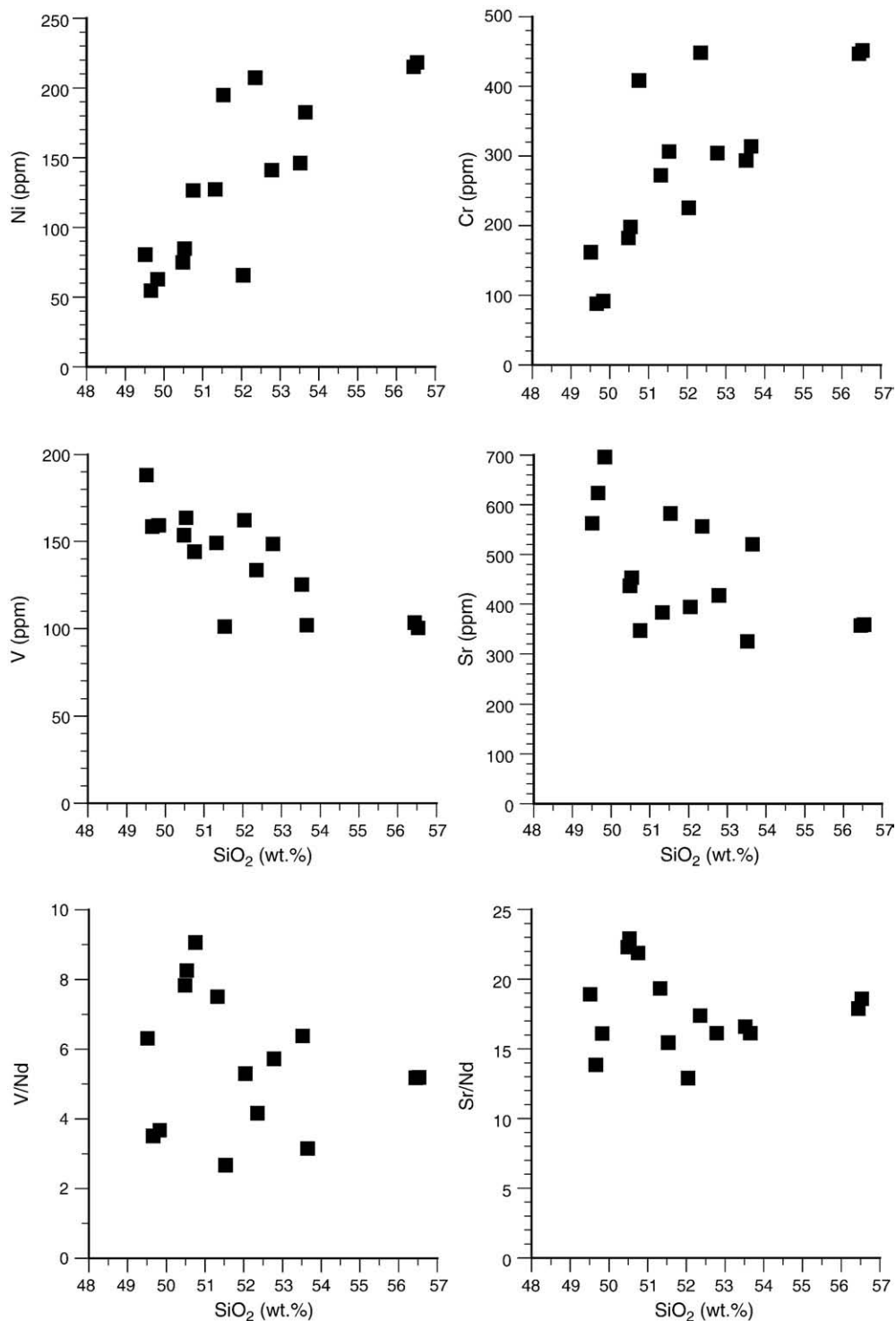


Fig. 5. Compatible trace element variations of Hirado-Seto samples.

than 1050 °C at 1 GPa (Hirose, 1997). On the other hand, the temperature of hydrous primitive basalts with SiO<sub>2</sub> < 51 wt.% would be higher than 1200 °C (Hirose and Kawamoto, 1995). Therefore, even if associated basalts are hydrous, the SCIM model requires a temperature difference greater than 150 °C at an identical pressure to form a basalt–HMA association. If associated basalts were anhydrous, the temperature of the primitive NW Kyushu basalts was 1300 °C at 1 GPa (Higo and Mashima, 2004; Mashima, 2005). Pyroxene thermometry for mantle xenoliths in the basalts also indicates that the maximum temperature of the basalts was 1300 °C (Arai et al., 2001). Thus, 150 °C would be the minimum estimate of the temperature difference

between HMA magmas and basalt magmas at 1 GPa. The SCIM model, therefore, requires a large temperature variation in the mantle at an identical pressure beneath Hirado-Seto.

According to previous high pressure melting experiments of peridotites, the MgO contents of the samples indicate relatively high degrees of melting, such as 5–10%. Liquid droplets formed by partial melting of the mantle segregate and gather to form a chamber prior to eruptions. Therefore, the temperature of a primitive magma represents that of a relatively wide area of the source mantle. H<sub>2</sub>O contents in primitive melts could widely vary, since H<sub>2</sub>O could be originally localized in hydrous phases in the source. Temperature of the mantle,

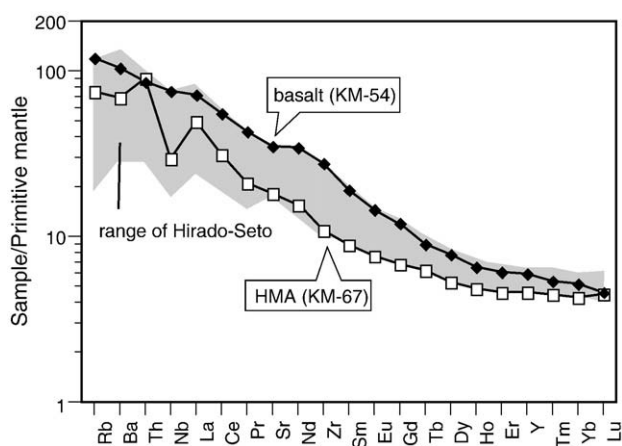


Fig. 6. Relative abundance diagrams for incompatible trace elements in Hirado-Seto samples. The compositions of pyrolite are from McDonough and Sun (1995).

however, could not widely vary at the same pressure in a given locality, since heat conduction in the mantle leads to a gradual variation in temperature. When the source involves primitive melts, the latent heat effect of partial melting also leads to a small temperature variation. Therefore, Shimoda et al. (1998) concluded that a mechanism for creating such a large temperature variation is an important but unsolvable issue with respect to the SCIM model for the generation of the basalt–HMA association.

In order to explain the high Ni feature of HMAs from the central Mexican Volcanic Belt, Straub et al. (2008) proposed that HMA magmas were formed by partial melting of pyroxenite. The pyroxenite source is formed by reaction between olivine in peridotites and  $\text{SiO}_2$  in slab-derived fluids. Petrologic examinations using the normative olivine–quartz–[Jd+CaTs] diagram, however, suggest that the reaction pyroxenite source could not form HMA magmas at pressures greater than 1 GPa under anhydrous conditions.

For pyroxenite systems involving opx, there are two thermal divides at high pressures, the plagioclase–opx (low Ca pyroxene) thermal divide between 1 and 2 GPa, and the garnet–opx thermal divide at pressures greater than 2 GPa (e.g., Baker and Eggler, 1987; Kogiso et al., 2004). These thermal divides are represented by the [Ab + An]–Hy tie line, and the [Jd+CaTs]–Hy tie line on the diagram (Fig. 10a). In order to form HMA magmas that plot on the Qtz excess side of the [Ab+An]–Hy tie line, reaction pyroxenite should at least plot on the Qtz excess side of the [Jd+CaTs]–Hy tie line of the diagram. The normative compositions of the reaction pyroxenite, however, could not cross over the [Jd+CaTs]–Hy tie line, since olivine in the original peridotite is consumed when the composition of the reaction product reaches the tie line.

The above conclusion is consistent with the compositions of natural pyroxenites. Many pyroxenites plot along the garnet–pyroxene thermal divide and/or on the quartz deficient side (Kogiso et al., 2004). Some pyroxenites show excess quartz, but such pyroxenites are regarded not as reaction pyroxenites but as cumulates.

Straub et al. (2008) proposed that reaction pyroxenite is composed of opx and cpx. Such a pyroxenite plots on the Hy point on the normative projection. If this is the case, partial melts of reaction pyroxenite plot along the tie line of [Jd + CaTs] and Hy (Fig. 10b, c).

In order to form HMA magmas under anhydrous conditions, reaction pyroxenite needs additional felsic components such as felsic veins. Additions of felsic veins, however, reduces the Ni contents of the hybrid of reaction pyroxenite and felsic veins, thus HMA magmas with high Ni could not be formed from the hybrid source. In conclusion, reaction pyroxenite is not able to form HMA magmas with high Ni contents at pressures greater than 1 GPa under anhydrous conditions.

In order to form HMA magmas with high Ni, reaction pyroxenite should be hydrous since the olivine primary field expands under

hydrous conditions at high pressures (Baker and Eggler, 1987). Addition of  $\text{H}_2\text{O}$ , however, leads to an insoluble thermal problem because  $\text{H}_2\text{O}$  lowers the solidus temperature of reaction pyroxenite. The reaction pyroxenite model, therefore, is inadequate to explain the genesis of the basalt–HMA magmas at Hirado-Seto.

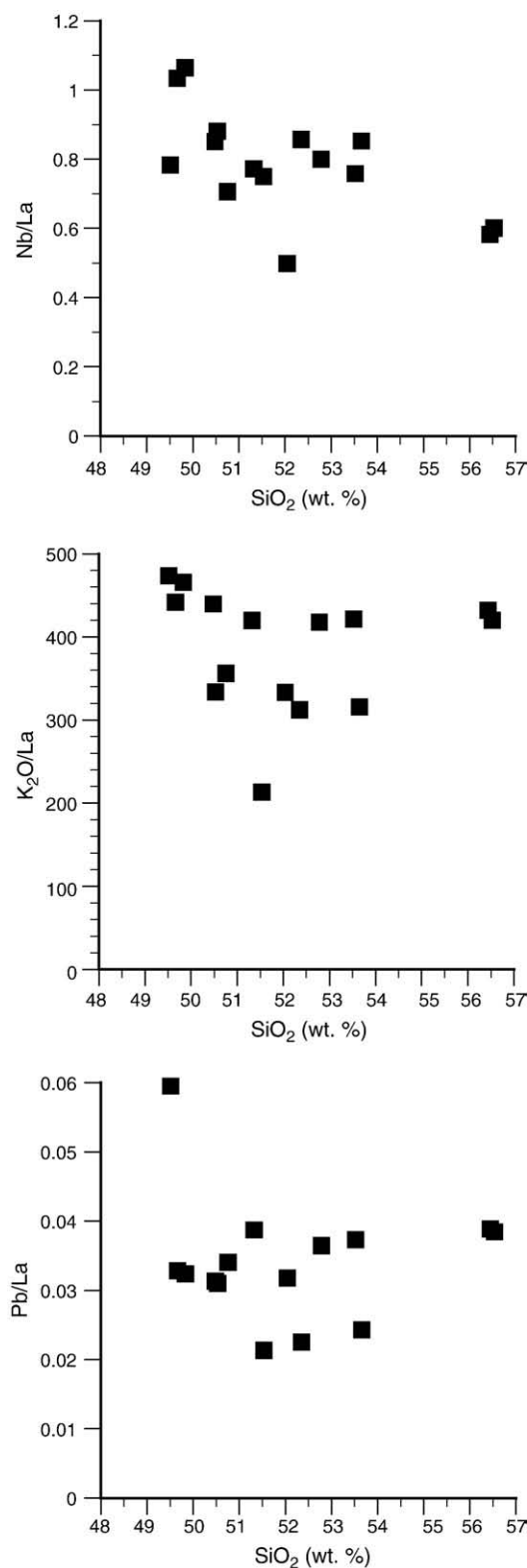
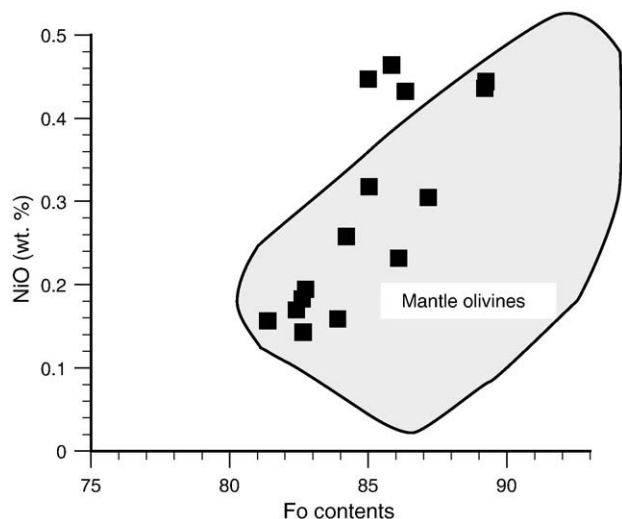


Fig. 7. Variations of Nb/La,  $\text{K}_2\text{O}/\text{La}$  and Pb/La against  $\text{SiO}_2$ . The lack of systematic relationships between these trace element ratios and  $\text{SiO}_2$  indicate that slab-derived components did not play a significant role in the Hirado-Seto magma genesis.



**Fig. 8.** Mg–Fe–Ni compositions for calculated olivine equilibrated with the bulk rock compositions of the Hirado-Seto samples. The calculation procedure is described in Higo and Mashima (2004). Compositions of mantle olivines are from Sobolev et al. (2005).

Geochemical features of the Hirado-Seto basalt–HMA association indicate that slab-derived hydrous components did not play a significant role in their petrogenesis. Based on geochemical modeling, Tatsumi and Hanyu (2003) proposed that the Setouchi HMA magmas, SW Japan, involved partial melts of altered oceanic crust. As with Setouchi, the Shikoku Basin is part of the Philippine Sea plate which is subducting to the north under Kyushu. The Shimanto accretional belt, a prime candidate for the source of the sediment components in the Setouchi source, constitutes fore-arc Kyushu. If slab-derived components played significant roles in the genesis of Hirado-Seto HMAs, geochemical features similar to the Setouchi HMAs would be observed in them.

A relative depletion in Nb is considered to be strong evidence for a significant role of slab-derived hydrous melts in the Setouchi HMA magma genesis (Tatsumi et al., 2001; Tatsumi and Hanyu, 2003). Nb/La of the Hirado-Seto HMA is 0.6 and is a little lower than that of basalts ranging from 1.1 to 0.7. If the low Nb/La of the HMA is the result of contributions of fluids derived from subducting altered oceanic crust and/or sediments,  $K_2O/La$  and/or  $Pb/La$  should show positive correlations with  $SiO_2$ .  $K_2O/La$  and  $Pb/La$  of the Hirado-Seto samples, however, do not show systematic correlations with  $SiO_2$  (Fig. 7). Therefore, geochemical features indicate that hydrous components derived from altered oceanic crust and/or sediments did not play an essential role in the genesis of the Hirado-Seto magmas.

Unaltered oceanic crust has low  $K_2O/La$ . Therefore, hydrous fluids derived from unaltered oceanic crust could have contributed to the Hirado-Seto magmatism. Unaltered oceanic crust, however, does not have any hydrous phase that brings  $H_2O$  into the mantle. In order to bring  $H_2O$  into the mantle, the subducting oceanic crust should be altered. Geochemical features of the Hirado-Seto samples, therefore, indicate an insignificant role for slab-derived components in their petrogenesis.

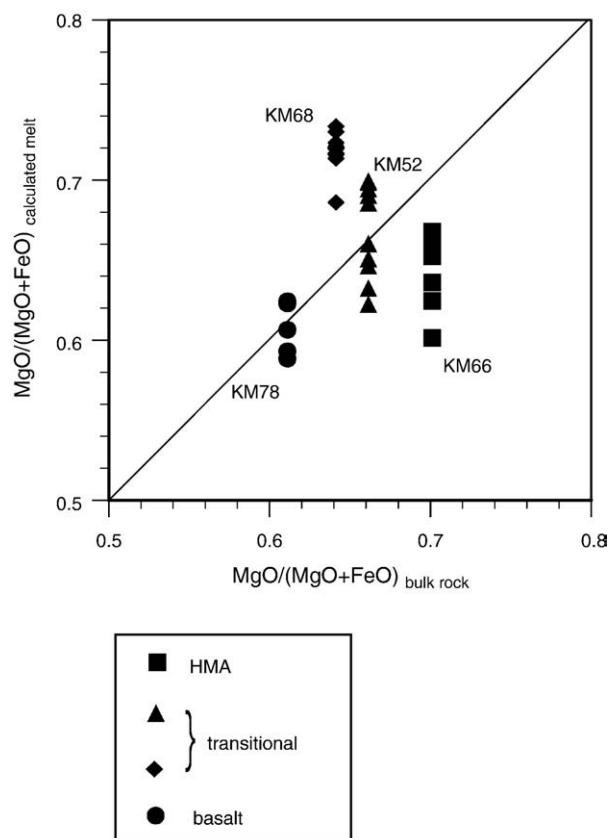
Based on thermodynamic calculations, Iwamori (2007) proposed that the dehydration of the subducting Shikoku Basin forms  $H_2O$ -rich regions with aqueous fluids and melts not beneath the back-arc area but beneath the volcanic front in the fore-arc area in present day North Kyushu. When Hirado-Seto magmatism occurred at 7 Ma, the subducting Shikoku Basin was younger and hence hotter than it is today. The Shikoku Basin dehydration would have occurred at pressures lower than present day. The subducting Shikoku Basin, therefore, would not have provided significant amounts of  $H_2O$  for the NW Kyushu mantle at 7 Ma.

HMA magmatism in subduction zones is generally believed to be caused by hydrous components derived from the subducting slab. In the case of Hirado-Seto, however, the SCIM model needs some modifications in order to explain the genesis of the basalt–HMA association.

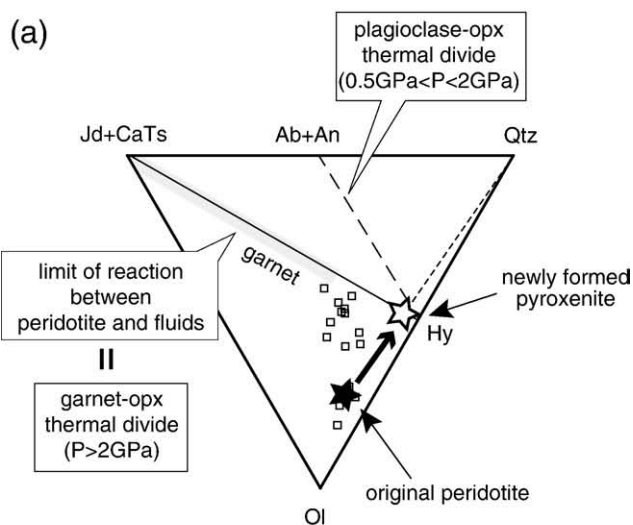
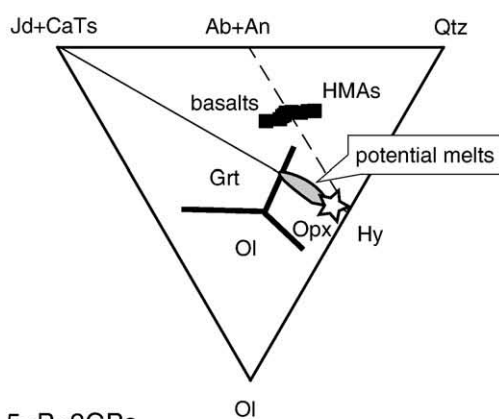
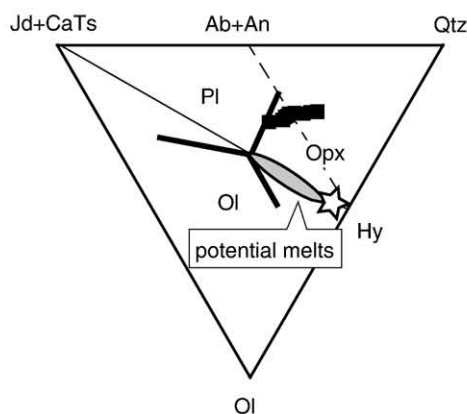
### 5.3. The MSPM model

Results of high pressure melting experiments of peridotites indicate that partial melting of anhydrous mantle at pressures less than 1 GPa could also form HMA magmas (Jaques and Green, 1980; Falloon et al., 1988; Kushiro, 1996). Falloon et al. (1988) proposed a model of multi-stage partial melting (MSPM) of relatively anhydrous mantle to explain the genesis of basalt–HMA associations in intra-oceanic island arc settings. They proposed that a first-stage melting process at a pressure of ~1 GPa would form basalt magmas, and that the residual mantle from this partial melting, after further upwelling, would partially melt to form HMA magmas. On the normative basalt tetrahedron projected on the  $[Jd+CaTs]$ –olivine–quartz base from cpx, the Hirado-Seto samples plot between the 1 GP and 0.5 GPa cotectics (Fig. 11). The normative compositions, therefore, suggest that these magmas could be formed at 1–0.5 GPa by partial melting of their sources.

As discussed above, the SCIM model needs a mechanism to create a large temperature variation at an identical pressure to form the basalt–HMA association. The advantage of the MSPM model is there is no necessity for such a mechanism. In Fig. 11, the normative compositions of the Hirado-Seto samples plot along a mantle adiabat at 1300 °C assuming anhydrous conditions. Partial melting of peridotite occurs along the adiabat until clinopyroxene in the source mantle is consumed (Falloon et al., 1988). The normative compositions suggest that the MSPM model could explain how the HMA–



**Fig. 9.** Comparison of  $MgO/(MgO+FeO)$  in bulk rock to that of calculated melts in equilibrium with olivine phenocrysts.  $KD_{ol-melt}$  is assumed to be 0.32.  $Fe^{2+}/(Fe^{2+}+Fe^{3+})$  of analyzed samples is assumed to be 0.8.

(b)  $P > 2\text{GPa}$ (c)  $0.5 < P < 2\text{GPa}$ 

**Fig. 10.** Petrologic examination of the reaction pyroxene source model for the genesis of a basalt–HMA association using the normative olivine–quartz–[Jd+CaTs] diagram. (a) Compositional path for the products of reaction between olivine in a peridotite and  $\text{SiO}_2$  in fluids. The composition of the reaction pyroxenite does not cross the [Jd+CaTs]–Hy tie line representing the garnet–pyroxene thermal divide. Open squares are compositions of Type II garnet pyroxenites (Liu et al., 2005). (b) Relationships between pyroxenite compositions and partial melt compositions at high pressures, such as 2 GPa. Reaction pyroxenite on the Qtz depleted side /or on the garnet–pyroxenite thermal divide could not form andesitic melts. Phase relationships are from Kogiso et al. (2004). Solid squares are compositions of Hirado-Seto samples. (c) Relationships between pyroxenite compositions and partial melt compositions at pressures from 0.5 GPa to 2 GPa.

basalt association formed under an identical thermal regime. Thus, the MSPM model could explain the genetic relationship between the basalt magmas and the HMA magmas at Hirado-Seto.

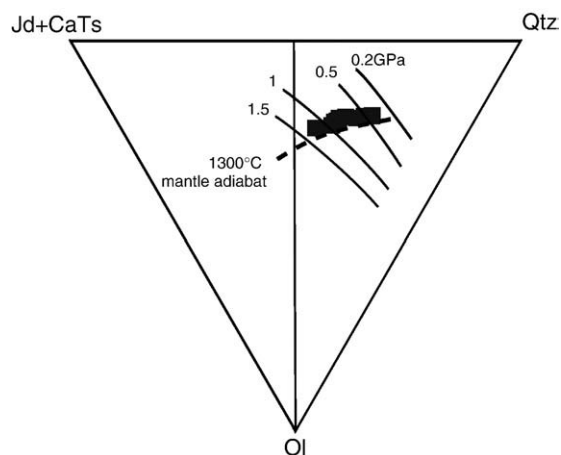


**Fig. 11.** The normative olivine–quartz–[Jd+CaTs] diagram for the Hirado-Seto samples. Cotectic lines and a 1300 °C mantle adiabat are from Falloon et al. (1988).

The HMAs are enriched in Ni and Cr compared with the basalts (Fig. 5). The MSPM model could explain these compatible element enrichments in the HMAs. Fig. 12 shows the correlation between Ni and Cr of the Hirado-Seto rocks. Their least squares regression line is  $\text{Ni} = 0.495\text{Cr}$ . The distribution coefficient of Ni between olivine and melt ( $D_{\text{Ni}}^{\text{ol-melt}}$ ) is ten to a thousand times greater than  $D_{\text{Cr}}^{\text{ol-melt}}$ .  $D_{\text{Ni}}^{\text{opx-melt}}$  and  $D_{\text{Ni}}^{\text{cpx-melt}}$  are the same order as  $D_{\text{Cr}}^{\text{opx-melt}}$  and  $D_{\text{Cr}}^{\text{cpx-melt}}$  (Green, 1994). Thus, the Ni–Cr correlation indicates that pyroxenes in the source mantle played a significant role in the Ni variation of Hirado-Seto magmas, as Straub et al. (2008) proposed for central Mexico.

On the normative [Jd+CaTs]–olivine–quartz diagram, a cotectic line for partial melting of peridotite shifts to the quartz apex as pressure decreases (Jaques and Green, 1980; Falloon et al., 1988). Hence, the relative contribution of orthopyroxene to the partial melt increases as pressure decreases. On the normative olivine–diopside–quartz diagram, the olivine/diopside ratio is similar for the basalts and HMAs (Fig. 13). The HMAs are enriched in the quartz components compared with the basalts, indicating that the HMAs are enriched in the orthopyroxene component compared to the basalts. Therefore, the behavior of orthopyroxene essentially controls the compositional differences between the basalts and the HMAs. The contribution of orthopyroxene to the melt formed at low pressures is greater than that at high pressures. Because of the large contribution of orthopyroxene,

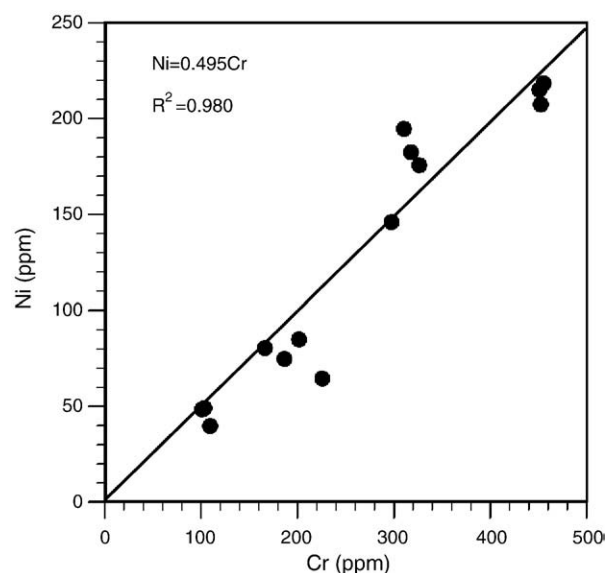


**Fig. 12.** Ni vs. Cr diagram for the Hirado-Seto samples.

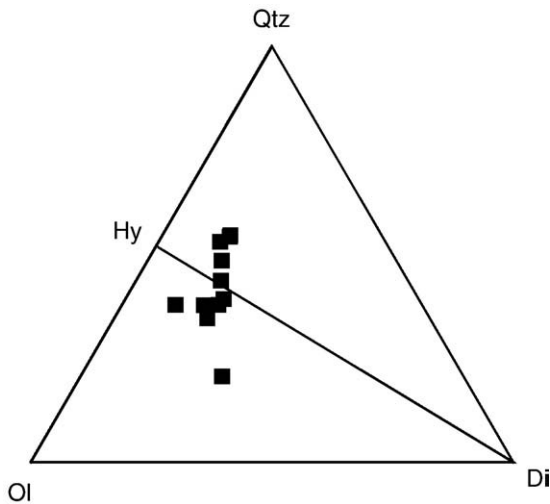


**Fig. 13.** Normative olivine–diopside–quartz diagram for the Hirado-Seto samples. The HMAs are enriched in the quartz component compared with the basalt samples, indicating that contributions of orthopyroxene to the HMA melt formation is larger than that to the basalt melt formation.

$D_{Ni}$  between the bulk source and melts at low pressures would be smaller than that at high pressures, which would have led to higher Ni concentrations in the HMAs compared to the basalts.

Olivine is a main reservoir of Ni in a peridotite. Therefore, it seems that a small contribution of olivine to the HMA melt leads to low Ni in HMAs. At pressures less than 2 GPa, however, spinel is another main reservoir of Ni in a peridotite. The volume of spinel is smaller than that of olivine in a peridotite. Spinel, however, is the first phase to disappear during partial melting of a peridotite. Therefore, Ni in the partial melt of a peridotite is essentially derived from spinel until it disappears in melting residues. The MSPM model indicates that the HMA magmas are finally separated from the source mantle at 0.5 GPa. At pressures lower than 1 GPa, phase transition from the spinel stability field to the plagioclase stability field would occur. Thus, the source mantle would not have had spinel when the HMA magma separated. Partial melting of the HMA source, however, would have started at pressures higher than 1 GPa where spinel is stable. Ni in the Hirado-Seto samples would have been mainly derived from spinel originally in their sources.

MSPM could also explain the geochemical features of the Hirado-Seto basalt–HMA association.  $K_2O/La$  and  $Pb/La$  of the basalt–HMA association indicate that the low  $Nb/La$  of the basalt–HMA association was the result of magmatic processes other than the addition of slab-derived hydrous components. Nb is compatible in Ti-oxides such as rutile (Green, 1994).  $TiO_2$  and  $P_2O_5$  show negative correlations with  $SiO_2$ , however,  $K_2O$  and  $Na_2O$  do not. This decoupling indicates that

Ti–P oxide minerals were involved in the low  $Nb/La$  ratio of the HMA. A possible explanation is precipitation of Ti–P oxides in the mantle under high  $fO_2$  conditions (Mashima, 2008c). An oxygen barometric study of mantle xenoliths in the NW Kyushu basalts younger than 4 Ma indicates that the  $fO_2$  of the uppermost mantle there would be from QFM–1 to QFM+1 at 1 GPa (Arai et al., 2001), which is higher than that of sub-oceanic mantle with an average of QFM–1.35 (Ballhaus, 1995). The normative compositions indicate that HMA magmas separated from their mantle source at pressures lower than basalt magma separations. The  $fO_2$  in the mantle decreases as pressure increases (Ballhaus, 1995). Thus, if MSPM formed the basalt–HMA association, the  $fO_2$  for HMA magma separation would be higher than that for basalt magma separation. Ti–P oxide minerals would have crystallized from HMA magmas during their ascent in the mantle under a high  $fO_2$  condition. Nb would have co-precipitated with Ti–P oxides and caused relative depletion of Nb. Thus, the relative depletion of Nb in the HMAs could be explained in the context of MSPM.

Assuming a homogeneous anhydrous source mantle, Falloon et al. (1988) proposed that HMA magmas are formed from melting residues of basalt magma formations. If this is the case, HMA magmas should be depleted in incompatible elements since incompatible elements in the mantle source are concentrated in partial melts, formed during the first stage of partial melting (Tatsumi, 1982). The Hirado-Seto HMAs, however, have incompatible element concentrations similar to those of the associated basalts. Thus, the HMA magmas were not derived from residues of basalt magma formations. Alternatively, the high incompatible element concentrations indicate that mantle source heterogeneity would have caused the variation in melt separation depths (Fig. 14). Solidus temperatures of peridotites depend on their  $FeO^*/MgO$ . A solidus temperature of a low  $FeO^*/MgO$  peridotite is higher than that of a high  $FeO^*/MgO$  peridotite (Falloon et al., 1988; Hirose and Kushiro, 1993).  $FeO^*/MgO$  of the HMA is lower than that of the basalt, indicating the solidus temperature of the HMA source was higher than that of the basalt source. Therefore, the pressure where the HMA source began partial melting would have been lower than the pressure where the basalt source began partial melting.

Assuming they were hydrous magmas, the basalt source would also have started earlier than the HMA source. As discussed above, significant  $H_2O$ -addition did not occur to the Hirado-Seto sources. Although it is impossible to evaluate original  $H_2O$  contents of Hirado-Seto rocks, Ce with a relative incompatibility similar to  $H_2O$  is an indicator of  $H_2O$ . The HMAs contain 52–54 ppm Ce, while the basalts contain 32–96 ppm Ce. The mean  $H_2O/Ce$  for Hawaii is evaluated to  $214 \pm 17$  (Dixon and Clague, 2001). The mean  $H_2O/Ce$  indicates that the HMAs and the basalts would have originally contained 1.1 wt.% and 0.7–2 wt.%  $H_2O$ . Basalts with higher Ce and  $FeO^*/MgO$  than those in the HMAs would have started partial melting earlier than the HMAs. Some basalts contain Ce lower than those in the HMAs. The lowest

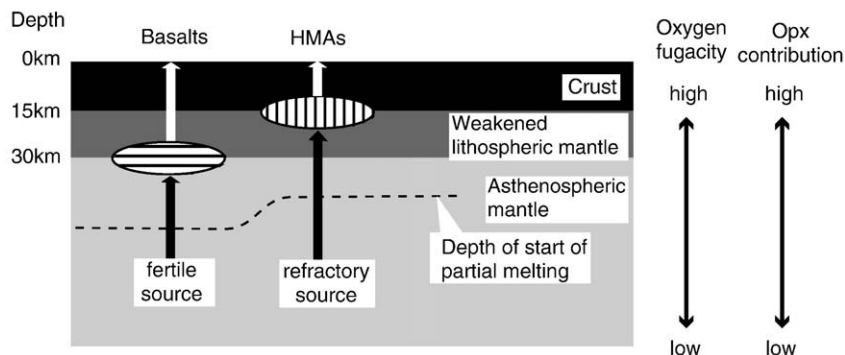


**Fig. 14.** Schematic model for the genesis of a basalt–HMA association at Hirado-Seto. Basalt magmas derived from a fertile source start melting at higher pressure in the mantle and separate from the source at 1 GPa. HMA magmas derived from a refractory source start melting at shallower depths in the mantle and separate from the source at 0.5 GPa. A high oxygen fugacity for the upper most mantle caused relative depletions of Nb in HMA magmas.

Ce (32 ppm) indicates that H<sub>2</sub>O in low Ce basalts would have been 0.4 wt.% lower than that in the HMAs at maximum. Since the difference of H<sub>2</sub>O was small, the basalt source with high FeO\*/MgO would also have started partial melting earlier than the HMA source with low FeO\*/MgO.

Melt productivity of the HMA source would have been lower than that of the basalt source. Because of low melt productivity, separation of HMA magmas from their source would have lagged behind basalt magma separation. Therefore, mantle source heterogeneity would have played an important role in the genesis of the basalt–HMA association at Hirado-Seto.

#### 5.4. Tectonic implications

It is generally believed that, in subduction zones, primitive magmas would finally separate from the mantle source at the Moho. Thus, the MSPM model indicates that the Moho depth at Hirado-Seto was 15 km when the basalt–HMA volcanism occurred at 7 Ma. Tectonic history of the Hirado-Seto magmatism is consistent with this petrological interpretation. In NW Kyushu, basin subsidence intermittently continued from the Paleogene to the early Miocene. Based on rheological modeling, the lower crust of NW Kyushu is considered to have been removed during basin subsidence (Nakada et al., 1997; Yamada and Nakada, 2006).

The Sea of Japan opened prior to the Hirado-Seto basalt–HMA volcanism. Geologic evidence, such as the right-lateral strike-slip structures along the Tsushima-Goto Fault between Kyushu and Korea and rapid sedimentation of the Nojima Group at Kita-Matsuura, indicate that SW Japan would have undergone a right-lateral displacement along the Tsushima-Goto Fault during the opening of the Sea of Japan (Itoh, 2001; Komatsubara et al., 2005; Mashima, 2008b). Since NW Kyushu is located on the back-arc side of SW Japan and at a suture zone between the Sea of Japan and the East China Sea, a right-lateral displacement of SW Japan caused strong transtensional tectonic stress. Hence, the crust of Hirado-Seto would have thinned during the opening of the Sea of Japan.

Nakada et al. (1997) and Yamada and Nakada (2006) proposed that solidification of basalt melts, accumulated at the Moho, thickened the NW Kyushu lithosphere before the start of volcanism. They, however, did not carry out detailed petrologic and geologic examinations to support this model. The model is inconsistent with petrologic observations such as small volumes of felsic volcanic rocks formed by crustal anatexis and/or high degree of fractional crystallization of basalt magmas (Mashima, 2006).

Petrological observations indicate that rigid lithospheric mantle would not have existed when the Hirado-Seto lavas erupted at 7 Ma. Relatively low Na<sub>2</sub>O in clinopyroxene in peridotite xenoliths included in basalt younger than 4 Ma indicates that the peridotites are low-pressure mantle restites (Arai et al., 2001). The NW Kyushu basalts younger than 4 Ma contain ultramafic xenoliths. The basalts older than 6 Ma contain only ultramafic xenocrysts (Ishibashi, 1970). After the opening of the Sea of Japan, the lithospheric mantle would have newly formed through cooling and inversion tectonics. These petrologic observations indicate that NW Kyushu would not have had rigid lithosphere before 4 Ma. NW Kyushu would have lacked rigid lithosphere when the basalt–HMA association erupted at Hirado-Seto at 7 Ma.

Hirado-Seto has geologic features similar to those of the Tertiary East China Sea Shelf basin (Okada, 1993). The present day average thickness of the East China Sea Shelf basin is estimated to be 30–22 km. The thickness of the active Okinawa Trough is estimated to be 14–20 km (Zhou et al., 1989). These estimates are consistent with the assumption that the lithosphere below Hirado-Seto was thinner than the present day lithosphere when the Hirado-Seto volcanism occurred. Lithospheric thinning during the opening of the Sea of

Japan, therefore, would have enabled HMA magma separation at abnormally low pressures.

Since  $fO_2$  of the mantle depends on depth. The shallow Moho would have led to high  $fO_2$  of the uppermost part of the mantle, which caused the low Nb/La of the HMAs. The lithospheric mantle represented by mantle xenoliths would have been newly formed by melt extraction and cooling after the Hirado-Seto magmatism. Thus, when the Hirado-Seto volcanism occurred, the  $fO_2$  of the uppermost mantle would have been higher than that recorded in mantle xenoliths.

Partial melting of a young oceanic lithosphere of the Shikoku Basin is believed to have played an essential role of HMA magma genesis at Setouchi, SW Japan, although it is unclear whether the slab extended to Setouchi or not during the Setouchi volcanism. The MSPM model indicates that hydrous components derived from the subducting Shikoku Basin did not play an essential role in the genesis of the Hirado-Seto basalt–HMA association. Seismic and geologic observations imply that the Shikoku Basin did not extend to NW Kyushu when the Hirado-Seto volcanism occurred.

Seismic observations indicate that the subducting Shikoku Basin does not extend to Hirado-Seto at present. The Shikoku Basin steeply subducts to Kyushu, and then vertically descends to deeper parts of the mantle on the oceanic side of the Kyushu volcanic front (Wang et al., 2004). In order to extend to NW Kyushu during the basalt–HMA magmatism, the Shikoku Basin should have gently subducted to Kyushu. Gentle subduction would cause strong mechanical coupling between a subducting plate and an overriding plate. In the case of the Setouchi district, SW Japan, where the Shikoku Basin gently subducts at the present day, strong compressive tectonics occurred on the back-arc side during the opening of the Sea of Japan prior to Setouchi magmatism at 14 Ma. On the back-arc side of the Setouchi district, sedimentary rocks were tightly folded with E–W axes simultaneously with their sedimentation during the opening of the Sea of Japan (Yamauchi and Yoshitani, 1992). In NW Kyushu, however, the Nojima Group which was deposited during the opening of the Sea of Japan does not show a folded structure. Its high subsidence ratio indicates

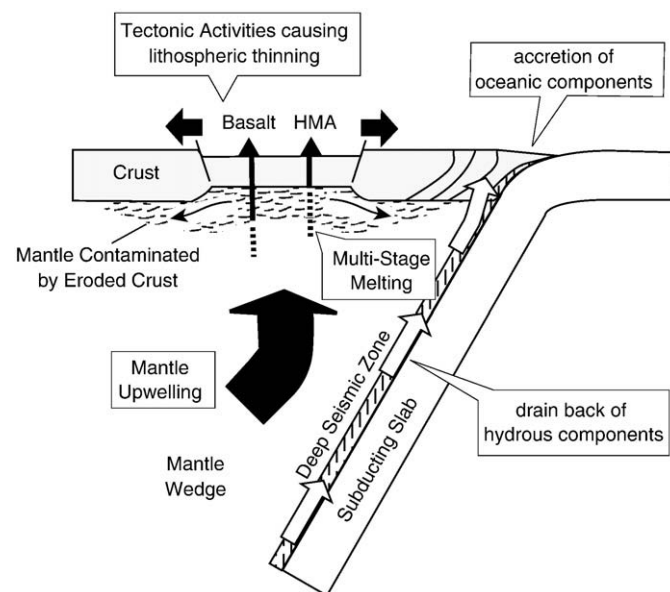


**Fig. 15.** A schematic model for the genesis of a basalt–HMA association in the context of the geodynamics of a subduction zone. In the model, slab-derived hydrous components drain back along the deep seismic zone at the mantle/slab boundary. The crust, including accreted components, is eroded by extensional tectonic activities. The uppermost part of the mantle wedge is contaminated by the eroded crust. HMA magmas formed in the shallower part of the mantle involve accreted oceanic components in the eroded crust. Basalt magmas formed in the deeper part of the mantle involve less eroded accretional oceanic components.

that transtensional strain dominated NW Kyushu at that time (Komatsubara et al., 2005). These contrasting tectonic styles between NW Kyushu and the back-arc area of the Setouchi district indicate that mechanical coupling between the overriding plate and the subducting plate was weak at NW Kyushu, suggesting that the Shikoku Basin would already be steeply subducting during the opening of the Sea of Japan.

##### 5.5. Implications for basalt–HMA magmatism in global subduction zones

Previous SCIM models emphasize the role of hydrous components derived from the subducting slab in the genesis of basalt–HMA magmatism in subduction zones. The SCIM models, however, have an unsolvable thermal problem to explain the genesis of a basalt–HMA association in each locality. The MSPM model could resolve the thermal problem as discussed above. The MSPM model, however, seems to not be able to explain the geochemical features of subduction zone HMAs that were attributed to hydrous components derived from subducting slabs in SCIM models.

In subduction zones, deep earthquakes occur along the mantle/slab boundary above subducting altered oceanic crust (Tsuji et al., 2008; Van Avendonk et al., 2008), indicating that the mantle/slab boundary is a weak fault zone filled by cracks. Channel flow through cracks in the deep seismic zone would transport slab-derived hydrous fluids to the surface more efficiently than porous flow in the wedge mantle. Fluids derived from a slab would effectively drain back to a frontal arc area through the deep seismic zone (Fig. 15). Therefore, the input of slab-derived hydrous components into the wedge mantle would be significantly smaller than that assumed by the SCIM models.

Accretion of subducting oceanic components to the overriding plate characterizes subduction zone tectonics. In an inner-arc area, regional mantle upwelling during intra-arc magmatism and/or intra-arc basin formation would erode accreted oceanic components from the crust (e.g., Nakada et al., 1997). Some portions of eroded crust would partially melt and assimilate with the uppermost part of the wedge mantle. These tectonic activities would enrich the uppermost mantle in slab-derived components. The MSPM model places the HMA source at shallower depth than the basalt source. Therefore, geochemical features of the ordinary basalt–HMA association in subduction zones could be explained in the context of the MSPM model.

In both the Western and Eastern Pacific areas, vigorous granitic magmatism occurred in the Cretaceous. For example, the basement of the Setouchi district, SW Japan, is the Ryoke Belt, comprised of Cretaceous granites and accretional materials that have undergone high temperature metamorphism (Banno and Nakajima, 1991). The basement underlying Mt Shasta in the Cordilleran System accreted during the Phanerozoic, and granitic magmatism occurred in the Cretaceous (Barton, 1996). Accreted oceanic material would have contaminated the uppermost part of the mantle beneath these areas during these magmatic events. Geochemical features of these HMAs could also be explained by involvement of the uppermost mantle that was contaminated by accretionary components.

The SCIM models for subduction zone HMAs assumed that the crust beneath volcanoes is thicker than 30 km. The crustal thickness beneath volcanoes, however, is not well known, because a significant seismic discontinuity is not observed. Regional mantle upwelling causing magmatism could locally erode and thin the crust. In several HMA localities, strike-slip tectonics are developed. For example, the central Mexican Volcanic Belt is developed along the Tenago Fault characterized by transtensional left-lateral strike-slip movements (Bellotti et al., 2006). The western Aleutian arc is a typical strike-slip shear zone caused by oblique subduction of the Pacific Plate (Yogodzinski et al., 1994). Transtensional strain could cause crustal thinning and elevation of the Moho to shallow depths in these areas. In the case of the Setouchi district, the crustal thickness at the time of

volcanism would have been thinner than the present day, as the crust of the Setouchi district was horizontally shortened by late Miocene inversion tectonics that occurred after the volcanism (Itoh and Nagasaki, 1996).

Previous SCIM models ignored the roles of oceanic components accreted to the overriding plate. The SCIM models ignored mechanical and chemical interactions between the mantle and the crust involving accreted components. Subduction zone tectonics, however, indicate that the crust would interact mechanically and chemically with the uppermost part of the mantle. Basalt–HMA associations formed by MSPM, therefore, could be associated with many subduction zones.

## 6. Conclusion

An association of basalts and high magnesium andesites is found at Hirado-Seto in NW Kyushu, SW Japan. The association was erupted at 7–6 Ma, following the opening of the Sea of Japan. The hydrous slab component-induced model cannot explain the genesis of the Hirado-Seto magmas, since the model requires an unrealistic temperature variation in the mantle at an identical pressure. Geochemical features, such as a lack of a positive  $K_2O/La-SiO_2$  correlation, support this interpretation. The normative olivine–quartz–[Jd + CaTs] compositions indicate that the Hirado-Seto magmas were formed by multi-stage partial melting of a heterogeneous source mantle at pressures ranging from 1 to 0.5 GPa along a 1300 °C mantle adiabat assuming anhydrous conditions. Basalt magmas separated from the source at 1 GPa. High magnesium andesite magmas separated from the source at 0.5 GPa. Lithospheric thinning caused by strong transtensional strain during the opening of the Sea of Japan would have enabled HMA magma separation at low pressure.

Subduction zone tectonics, such as accretion of oceanic materials to overriding plates and intra-arc basin formations, indicates that the multi-stage partial melting model could also explain the genesis of basalt–HMA associations in other subduction zones.

## Acknowledgements

I thank N. Nakatsuka, K. Umeda, E. Sasao, and Kakamu at Tono Geoscience Center, Japan Atomic Energy Agency and M. Watanabe at Center of Advanced Instrumental Analysis, Kyushu University, for their support in this study. I thank S. Straub for helpful discussions with me. Comments by two anonymous reviewers greatly improved the manuscript. I am grateful to G. N. Eby for his helpful comments and kind corrections of the manuscript. I am also grateful to T. D. Tindell for his kind corrections of the manuscript. Several figures in this paper were produced using General Mapping Tool written by Wessel and Smith (1998).

## References

- Arai, S., Abe, N., Hirai, H., Shimizu, Y., 2001. Geological, petrographical and petrological characteristics of ultramafic–mafic xenoliths in Kurose and Takashima, northern Kyushu, southwestern Japan. *Science reports of the Kanazawa University*, vol. 46, pp. 9–38.
- Baker, D.R., Eggler, D.H., 1987. Compositions of anhydrous and hydrous melts coexisting with plagioclase, augite, and olivine or low-Ca pyroxene from 1 atm to 8 kbar: application to the Aleutian volcanic center of Atka. *American Mineralogist* 72, 12–28.
- Ballhaus, C., 1995. Is the upper mantle metal-saturated? *Earth and Planetary Science Letters* 132, 75–86.
- Banno, S., Nakajima, T., 1991. Metamorphic belts of Japan. *Episodes* 14, 280–285.
- Barton, M.D., 1996. Granitic magmatism and metallogeny of southwestern North America. *Granitic magmatism and metallogeny of southwestern North America. Transactions of the Royal Society of Edinburgh: Earth Sciences* 87, 261–280.
- Bellotti, F., Capra, L., Groppelli, G., Norini, G., 2006. Tectonic evolution of the central-eastern sector of Trans Mexican Volcanic Belt and its influence on the eruptive history of the Nevado de Toluca volcano (Mexico). *Journal of Volcanology and Geothermal Research* 158, 21–36.
- Bourdon, E., Eissen, J., Gutscher, M.A., Monzier, M., Hall, M.L., Cotten, J., 2003. Magmatic response to early aseismic ridge subduction: the Ecuadorian margin case (South America). *Earth and Planetary Science Letters* 205, 123–138.

- Dixon, J.E., Clague, D.A., 2001. Volatiles in basaltic glasses from Loihi Seamount, Hawaii: evidence for a relatively dry plume component. *Journal of Petrology* 42, 627–654.
- Falloon, T.J., Green, D.H., Hatton, C.J., Harris, K.L., 1988. Anhydrous partial melting of a fertile and depleted peridotite from 2–30 kb and application to basalt petrogenesis. *Journal of Petrology* 29, 1257–1282.
- Falloon, T.J., Green, D.H., O'Neill, H.S.C., Hibberson, W.O., 1997. Experimental tests of low degree peridotite partial melt compositions: implications for the nature of anhydrous near-solidus peridotite melts at 1 GPa. *Earth and Planetary Science Letters* 152, 149–162.
- Falloon, T.J., Green, D.H., Danyushevsky, L.V., Faul, U.H., 1999. Peridotite melting at 1.0 and 1.5 GPa: an experimental evaluation of techniques using diamond aggregates and mineral mixes for determination of near-solidus melts. *Journal of Petrology* 40, 1343–1375.
- Green, T.H., 1994. Experimental studies of trace-element partitioning applicable to igneous petrogenesis—Sedona 16 years later. *Chemical Geology* 117, 1–36.
- Grove, T.L., Parman, S.W., Bowring, S.A., Price, R.C., Baker, M.B., 2002. The role of an H<sub>2</sub>O-rich fluid component in the generation of primitive basaltic andesites and andesites from the Mt. Shasta region, N California. *Contributions to Mineralogy and Petrology* 142, 375–3396.
- Higo, T., Mashima, H., 2004. Thermal state of northwest Kyushu mantle suggested by the petrochemistry of the Tara-dake basalts. *Geophysical Research Letters* 31, L03604.
- Hirose, K., 1997. Melting experiments on Iherzolite KLB-1 under hydrous conditions and generation of high-magnesian andesitic melts. *Geology* 25, 42–44.
- Hirose, K., Kushiro, I., 1993. Partial melting of dry peridotites at high pressures: determination of compositions of melts segregated from peridotite using aggregates of diamond. *Earth and Planetary Science Letters* 114, 477–489.
- Hirose, K., Kawamoto, T., 1995. Hydrous partial melting of Iherzolite at 1 GPa: the effect of H<sub>2</sub>O on the genesis of basaltic magmas. *Earth and Planetary Science Letters* 133, 463–473.
- Ichikawa, K., 1972. Constraints for the reconstruction of the Sea of Japan: evidence from geologic relationships between Southwest Japan and the Korean Peninsula in Paleozoic–Mesozoic periods. *Kagaku Science* 42, 630–633 (in Japanese).
- Inoue, E., 1982. Geologic issues of cretaceous and tertiary sedimentary rocks on either Bank of the Tsushima Strait II: offshore geology and synthesis. *Chishitsu News* 340, 46–61 (in Japanese).
- Ishibashi, K., 1970. Petrochemical study of basic and ultrabasic inclusions in basaltic rocks from northern Kyushu, Japan. *Memoirs of the Faculty of Science, Kyushu University. Series D, Geology* 20, 85–146.
- Ishida, M., Sakamashi, M., 2003. The configuration of the Philippine Sea slab: from the Kanto district to the Kyushu district in Japan. *Chikyū Monthly* 25, 168–172 (in Japanese).
- Itoh, Y., 2001. A Miocene pull-apart deformation zone at the western margin of the Japan Sea back-arc basin: implications for the back-arc opening mode. *Tectonophysics* 334, 235–244.
- Itoh, Y., Nagasaki, Y., 1996. Crustal shortening of Southwest Japan in the Late Miocene. *Island Arc* 5, 337–353.
- Iwamori, H., 2007. Transportation of H<sub>2</sub>O beneath the Japan arcs and its implications for global water circulation. *Chemical Geology* 293, 182–198.
- Jaques, A.L., Green, D.H., 1980. Anhydrous melting of peridotite at 0–15 Kbar pressure and the genesis of tholeiitic basalts. *Contributions to Mineralogy and Petrology* 73, 287–310.
- Jenner, G.A., 1982. Petrogenesis of high-Mg Andesites: an experimental and geochemical study with emphasis on high-Mg andesites from Cape Vogel, Papua New Guinea. PhD Theme, University of Tasmania.
- Jolivet, L., Tamaki, K., Fournier, M., 1994. Japan Sea, opening history and mechanism: a synthesis. *Journal of Geophysical Research* 99, 22237–22259.
- Kakubuchi, S., Nago, T., Kagami, H., 1994. Genetic relationship between tholeiite and alkaline basalts of the Kitamatsuura basalts, northwestern Kyushu, Japan. *Journal of Mineralogy, Petrology and Economic Geology* 89, 41–55 (in Japanese with English abstract).
- Kay, R.W., 1978. Aleutian magnesian andesites: melts from subducted Pacific Ocean crust. *Journal of Volcanology and Geothermal Research* 4, 117–132.
- Kelemen, P.B., 1995. Genesis of high Mg# andesites and the continental crust. *Contributions to Mineralogy and Petrology* 120, 1–19.
- Kimura, J., Stern, R.J., Yoshida, T., 2005. Reinitiation of subduction and magmatic responses in SW Japan during Neogene time. *Geological Society of America Bulletin* 117, 969–986.
- Kogiso, T., Hirschmann, M.M., Pertermann, M., 2004. High-pressure partial melting of mafic lithologies in the mantle. *Journal of Petrology* 45, 2407–2422.
- Komatsubara, J., Ugai, H., Danbara, T., Iwano, H., Yoshioka, T., Nakajima, T., Kano, K., Ogawawara, K., 2005. Fission-track age and inferred subsidence rate of the Lower to Middle Miocene Nojima Group in NW Kyushu. *Journal of the Geological Society of Japan* 111, 350–360.
- Kurasawa, H., 1967. Petrology of the Kita-matuura basalt in the northwest Kyushu, southwest Japan. *Report of Geological Survey of Japan*, p. 108.
- Kurasawa, H., 1970. Relationship between the Sazagawa Thurst and the basalt flows in the Kumisaka Area North of Sasebo City, Nagasaki Prefecture (Part 1). *Reprints of Cooperative Research for Disaster Prevention* 22, 87–90 (in Japanese with English abstract).
- Kushiro, I., 1969. The system forsterite–diopside–silica with and without water at high pressures. *American Journal of Science* 267-A, 269–294.
- Kushiro, I., 1996. Partial melting of a fertile mantle peridotite at high pressures: an experimental study using aggregates of diamond. In: Basu, A., Harts, S. (Eds.), *Earth Processes: Reading the Isotopic Code*. AGU, pp. 109–122.
- Liu, Y., Gao, S., Lee, C.-T.A., Hu, S., Liu, X., Yuan, H., 2005. Melt–peridotite interactions: links between garnet pyroxenite and high-Mg# signature of continental crust. *Earth and Planetary Science Letters* 234, 39–57.
- Mashima, H., 2005. Partial melting controls of the NW Kyushu basalts from Saga-Futagoyama. *Island Arc* 14, 165–177.
- Mashima, H., 2006. Comment on “Stratigraphic architecture of sedimentary basin induced by mantle diapiric upwelling and eustatic event” by Yamada and Nakada [Tectonophysics 415 (2006) 103–121]. *Tectonophysics* 428, 105–106.
- Mashima, H., 2008a. Comments on regional variation of whole rock chemistry of the Miocene felsic igneous rocks in the Kii Peninsula, southwest Japan” by Shinjoe et al. [J. Geol. Soc. Japan, 113, 310–325]. *Journal of the Geological Society of Japan* 114 (in Japanese).
- Mashima, H., 2008b. Comment on “Evolution of the eastern margin of Korea: constraints on the opening of the East Sea (Japan Sea)” by Kim H.J. et al. [Tectonophysics 436 (2007) 37–55]. *Tectonophysics* 455, 104–105.
- Mashima, H., 2008c. Comments on Tomographic evidence for the mantle upwelling beneath southwestern Japan and its implications for arc magmatism” by J. Nakajima and A. Hasegawa [Earth Planet. Sci. Lett., 254 (2007), 90–105]. *Earth and Planetary Science Letters* 265, 320–321.
- Matsui, K., Furukawa, T., Sawamura, K., 1989. Geology of the Sasebo district. With Geological Sheet Map at 1:50,000. *Report Geol Surv Japan* 92 pp (in Japanese with English abstract).
- Matsumoto, Y., 1961. Older basalts and sanukitic rocks in the Kishima Area, Saga Prefecture, Japan. The reports of the Research Institute of Science and Industry, Kyushu University, vol. 29, pp. 1–25 (in Japanese).
- McDonough, W.F., Sun, S.-S., 1995. The composition of the Earth. *Chemical Geology* 120, 223–253.
- Murakoshi, T., 2003. Seismic structure of the crust and uppermost mantle beneath Kyushu as inferred from receiver function analysis. PhD. Theme, Kyushu University, 87 pp.
- Nakada, M., Yanagi, T., Maeda, S., 1997. Sedimentary basin formation followed by flood basalt volcanism in northwest Kyushu, Japan: implications for lower crustal erosion induced by mantle diapiric upwelling. *Earth and Planetary Science Letters* 146, 415–429.
- Okada, H., 1993. Relationship between sedimentary basins on the shelf area in the East China Sea and the Central Kyushu Rift Valley. *Memoirs of the Geological Society of Japan* 41, 163–173 (in Japanese with English abstract).
- Rudnick, R.L., 1995. Making continental crust. *Nature* 378, 571–578.
- Shimoda, G., Tatsumi, Y., Nohda, S., Ishizaka, K., Jahn, B.M., 1998. Setouchi high-Mg andesites revisited: geochemical evidence for melting of subducting sediments. *Earth and Planetary Science Letters* 160, 479–492.
- Shiomi, K., Obara, K., Sato, H., 2006. Moho depth variation beneath southwestern Japan revealed from the velocity structure based on receiver function inversion. *Tectonophysics* 420, 205–221.
- Sobolev, A.V., Hofmann, A.W., Sobolev, S.V., Nikogosian, I.K., 2005. An olivine-free mantle source of Hawaiian shield basalts. *Nature* 434, 590–597.
- Straub, S.M., LaGatta, A.B., Pozzo, A.L.M.D., Langmuir, C.H., 2008. Evidence from high-Ni olivines for a hybridized peridotite/pyroxenite source for orogenic andesites from the central Mexican Volcanic Belt. *Geochemistry Geophysics Geosystems* 9, 101029/2007G.
- Tatsumi, Y., 1982. Origin of high-magnesian andesites in the Setouchi volcanic belt, southwest Japan, II. Melting phase relations at high pressures. *Earth and Planetary Science Letters* 60, 305–317.
- Tatsumi, Y., Hanyu, T., 2003. Geochemical modeling of dehydration and partial melting of subducting lithosphere: toward a comprehensive understanding of high-Mg andesite formation in the Setouchi volcanic belt, SW Japan. *Geochemistry Geophysics Geosystems* 4, 101029/2003G.
- Tatsumi, Y., Ishikawa, N., Anno, K., Ishizaka, K., Itaya, T., 2001. Tectonic setting of high-Mg andesite magmatism in the SW Japan arc: K–Ar chronology of the Setouchi volcanic belt. *Geophysical Journal International* 144, 625–631.
- Tatsumi, Y., Shukuno, H., Sato, K., Shibata, T., Yoshikawa, M., 2003. The petrology and geochemistry of high-magnesian andesites at the western tip of the Setouchi Volcanic Belt. *Journal of Petrology* 44, 1561–1578.
- Tomita, T., 1958. Chemical distinctions between the three principal series of basaltic rocks. In: Ishikawa, T., Minato, M., Hunahashi, M., Hashimoto, S., Kobayashi, H. (Eds.), *Jubilee Publication in Commemoration of the Sixtieth Birthday of Professor Jun Suzuki*. Hokkaido University, pp. 193–211 (in Japanese).
- Tsujii, Y., Nakajima, J., Hasegawa, A., 2008. Tomographic evidence for hydrated oceanic crust of the Pacific slab beneath northeastern Japan: implications for water transportation in subduction zones. *Geophysical Research Letters* 35, 101029/2008G.
- Uto, K., Hoang, N., Matsui, K., 2004. Cenozoic lithospheric extension induced magmatism in Southwest Japan. *Tectonophysics* 393, 281–299.
- Van Avendonk, H.J.A., Holbrook, W.S., Lizaralde, D., Mora, D.M.M., Harder, S., Bullock, A.D., Alvarado, G.E., Ramírez, C.J., 2008. Seismic evidence for fluids in fault zones on top of the subducting Cocos plate beneath Costa Rica. *Nature* (in revision).
- Wang, K., Wada, I., Ishikawa, Y., 2004. Stresses in the subducting slab beneath southwest Japan and relation with plate geometry, tectonic forces, slab dehydration, and damaging earthquakes. *Journal of Geophysical Research* 109, B08304.
- Wernicke, B., 1985. Uniform-sense normal simple shear of the continental lithosphere. *Canadian Journal of Earth Sciences* 22, 108–125.
- Yamada, Y., Nakada, M., 2006. Stratigraphic architecture of sedimentary basin induced by mantle diapiric upwelling and eustatic event. *Tectonophysics* 415, 103–121.
- Yamaguchi, M., 1964. Petrological notes on sanukitoids. *Science reports, Department of Geology, Kyushu University*, vol. 7, pp. 131–138 (in Japanese with English abstract).

- Yamauchi, S., Yoshitani, A., 1992. Miocene tectonics of the southern Japan Sea and its adjacent area. *Memoirs of the Geological Society of Japan* 37, 311–326.
- Yanagi, T., Maeda, S., 1998. Magma evolution observed in the Matsuura basalts in northwest Kyushu, Japan: an example of high -pressure open system fractional crystallization in a refilled magma chamber near the crust–mantle boundary. *Physics of the Earth and Planetary Interiors* 107, 203–219.
- Yogodzinski, G.M., Volynets, O.N., Koloskov, A.V., Seliverstov, N.I., Matvenkov, V.V., 1994. Magnesian andesites and the subduction component in a strongly calc-alkaline series at Piip volcano, far western Aleutians. *Journal of Petrology* 35, 163–204.
- Zhou, Z.W., et al., 1989. Characteristics and tectonic evolution of the East China Sea. In: Zhu, X. (Ed.), *Chinese sedimentary basins*. Elsevier, pp. 165–179.